Hydraulic and Geochemical Framework of the Idaho National Engineering and Environmental Laboratory Vadose Zone

John R. Nimmo,* Joseph P. Rousseau, Kim S. Perkins, Kenneth G. Stollenwerk, Pierre D. Glynn, Roy C. Bartholomay, and LeRoy L. Knobel

ABSTRACT

Questions of major importance for subsurface contaminant transport at the Idaho National Engineering and Environmental Laboratory (INEEL) include (i) travel times to the aquifer, both average or typical values and the range of values to be expected, and (ii) modes of contaminant transport, especially sorption processes. The hydraulic and geochemical framework within which these questions are addressed is dominated by extreme heterogeneity in a vadose zone and aquifer consisting of interbedded basalts and sediments. Hydraulically, major issues include diverse possible types of flow pathways, extreme anisotropy, preferential flow, combined vertical and horizontal flow, and temporary saturation or perching. Geochemically, major issues include contaminant mobility as influenced by redox conditions, the concentration of organic and inorganic complexing solutes and other local variables, the interaction with infiltrating waters and with the contaminant source environment, and the aqueous speciation of contaminants such as actinides. Another major issue is the possibility of colloid transport, which inverts some of the traditional concepts of mobility, as sorbed contaminants on mobile colloids may be transported with ease compared with contaminants that are not sorbed. With respect to the goal of minimizing aquifer concentrations of contaminants, some characteristics of the vadose zone are essentially completely favorable. Examples include the great thickness (200 m) of the vadose zone, and the presence of substantial quantities of fine sediments that can retard contaminant transport both hydraulically and chemically. Most characteristics, however, have both favorable and unfavorable aspects. For example, preferential flow, as promoted by several notable features of the vadose zone at the INEEL, can provide fast, minimally sorbing pathways for contaminants to reach the aquifer easily, but it also leads to a wide dispersal of contaminants in a large volume of subsurface material, thus increasing the opportunity for dilution and sorption.

The thick, complex vadose zone at INEEL has been intensively studied for several decades. The characterization of its hydraulic and geochemical framework, primarily in terms of relevance to contaminant transport, provides a foundation for diverse topical investigations at the INEEL and at comparable sites around the world.

This paper describes the vadose zone at the INEEL with respect to characteristics important to hydraulic and geochemical transport processes. It emphasizes the southwestern portion of the INEEL where, because of potential contaminants in this area, some of the most intensive subsurface characterization efforts have been done (Fig. 1). A major source of these contaminants is the INEEL facility known as the Subsurface Disposal Area (SDA) for radioactive and other hazardous waste. As a result, the SDA and its nearby surroundings are the portion of the INEEL that has been most intensively studied with respect to hydraulic and geochemical issues. This paper reflects this emphasis, though where possible we have formulated generalizations to apply to most or all of the INEEL. This review is designed to complement that of Smith (2004). In terms of local-scale geologic framework, it picks up from Smith's presentation of tectonics, volcanism, and basalt characteristics; it emphasizes relatively small-scale features and their role in transport processes. We cover basic issues of transport-relevant characteristics as known mainly from investigations since the 1950s by relatively standard techniques.

Much material in this paper derives from a 1999 USGS panel review of DOE-contractor investigations related to existing and potential contaminant transport (Rousseau et al., 2004). It follows the series of USGS Reports on the INEEL subsurface by Barraclough and by Rightmire and Lewis between 1965 and 1987. These reports contain answers to many questions frequently asked by scientists and policy makers who are not necessarily aware of this body of work. An important characteristic of the present and earlier reports is their combined treatment of hydraulic and geochemical issues.

The vadose zone and aquifer consists of interbedded basalts and sediments (e.g., Smith, 2004). In this paper and elsewhere, the layers of sediments between basalt layers are called sedimentary interbeds. Much of the characterization here directly relates to geologically similar areas throughout the Snake River Plain.

Key issues of vadose zone contaminant transport include (i) travel times to the aquifer, both average or typical values and the range of values to be expected, and (ii) modes of contaminant transport, especially sorption processes. Some of the complicating factors are the hydraulic and geochemical effectiveness of natural barriers; flowpath directions ranging from horizontal to vertical; the diffuse or preferential nature of flow; the chemical nature of contaminants and subsurface media; and the various sources of water now in the subsurface, such as local precipitation, runoff, and horizontal flow from spreading areas or elsewhere. We emphasize the role of sedimentary interbeds, basalts fractured to vari-

J.R. Nimmo and K.S. Perkins, USGS, 345 Middlefield Rd., Menlo Park, CA 94025; J.P. Rousseau and L.L. Knobel, USGS, P.O. Box 2230, Idaho Falls, ID 83401; K.G. Stollenwerk, USGS, Box 25046, Denver Federal Center, Denver, CO 80225; P.D. Glynn, USGS, 12201 Sunrise Valley Drive, Reston, VA 20192; R.C. Bartholomay, USGS, 111 Kansas Ave SE, Huron, SD 57350. Received 18 Mar. 2003. Special Section: Understanding Subsurface Flow and Transport Processes at the Idaho National Engineering & Environmental Laboratory (INEEL) Site. *Corresponding author (jrnimmo@usgs.gov).

Published in Vadose Zone Journal 3:6–34 (2004).

677 S. Segoe Rd., Madison, WI 53711 USA

Abbreviations: CEC, cation exchange capacity; DOC, dissolved organic C; INEEL, Idaho National Engineering and Environmental Laboratory; INTEC, Idaho Nuclear Technology and Engineering Center; SDA, Subsurface Disposal Area; VZRP, Vadose Zone Research Park.

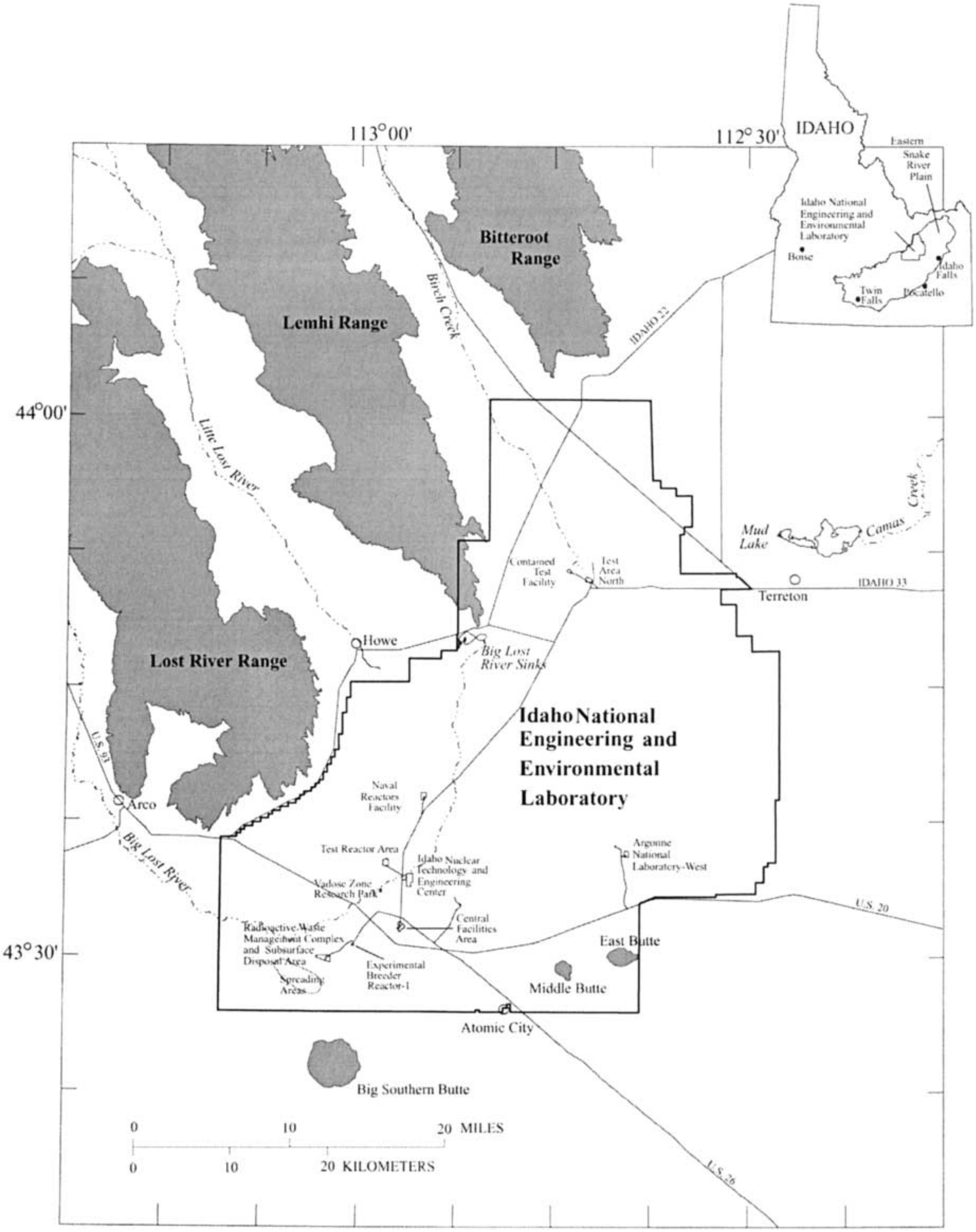

Fig. 1. Geographic features and selected facilities of the Idaho National Engineering and Environmental Laboratory and vicinity.

ous degrees, surficial materials, and the connections between the various media. A critical issue throughout is what scale has primary relevance, for example whether heterogeneity at the centimeter scale within sedimentary layers has significant effect relative to heterogeneity at the 10-m scale that would include both basalt and sediments.

HYDROLOGIC FRAMEWORK

Our current understanding of transport phenomena in the vadose zone at the INEEL is dominated by the great heterogeneity and anisotropy of this earth system, especially evident in the layering of highly dissimilar materials. The diversity of materials puts emphasis on several issues: multiple types of hydraulic pathways, pref-

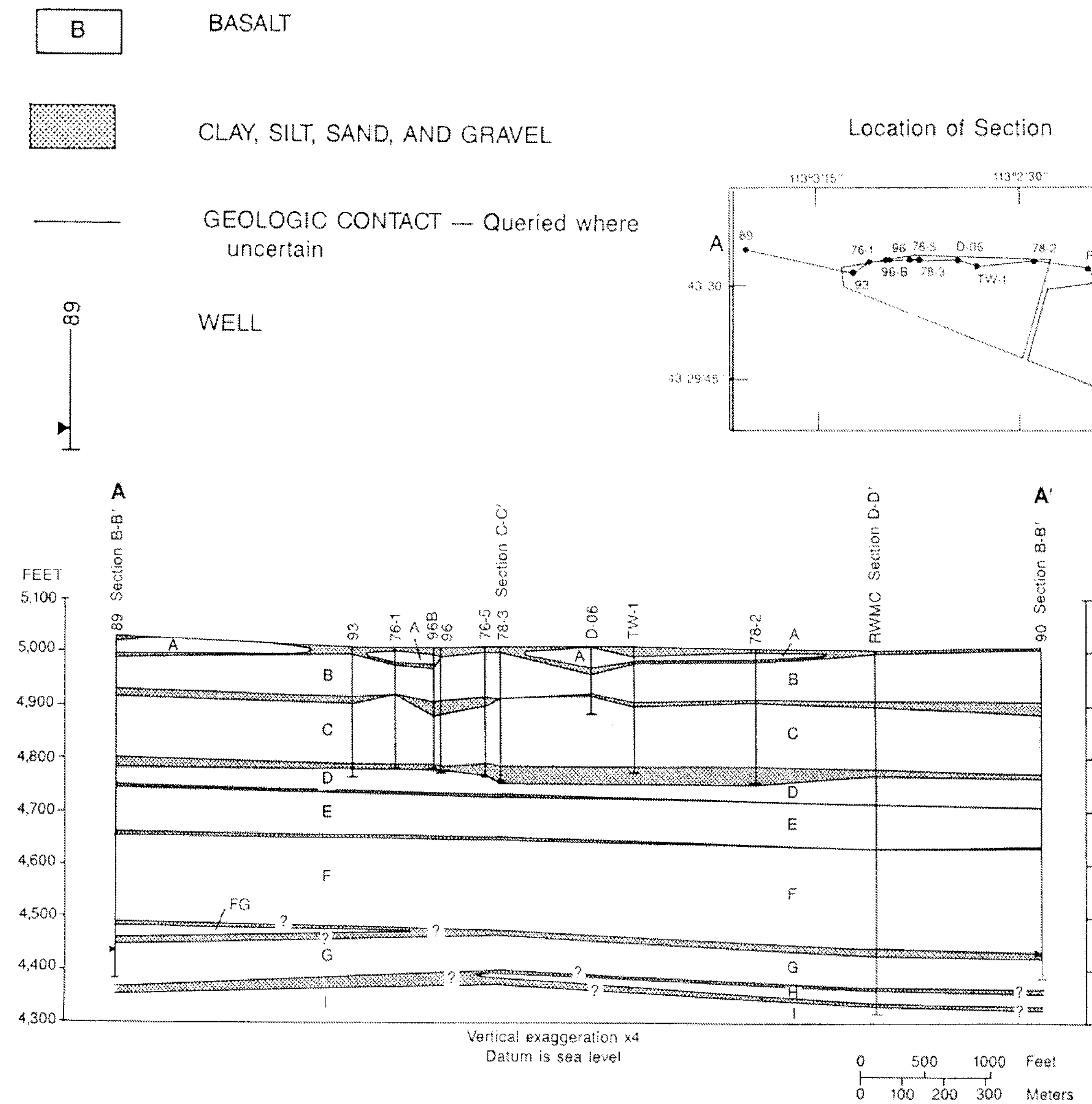

Fig. 2. Geologic cross section at the INEEL Subsurface Disposal Area, illustrating interbedded basalt flows and sediments.

erential flow, combined vertical and horizontal flow, and temporary saturation or perching.

The geology and hydrology of this site typify the eastern Snake River Plain. The surface vegetation is mostly sagebrush, rabbitbrush, and wheatgrass. There are topographic depressions, normally free of surface water but vulnerable to local flooding. The geologic framework has been characterized on the basis of data from hundreds of boreholes. Many continuous cores up to 550 m in length are available for inspection at the USGS core library (Davis et al., 1997). Recoveries of basalt in most of these cores have been essentially 100%. Recoveries of sediment have ranged from 0 to 100% and are commonly <50% (Hughes, 1993; Burgess et al., 1994). Borehole geophysical data from caliper, neutron, natural γ, γ–γ, and density measurements have been logged for most boreholes (Bartholomay, 1990c). The vadose zone, about 200 m thick near the SDA, overlies the Eastern Snake River Plain aquifer, which supplies about 2.5×10^9 m^3 yr^{-1} of water for agriculture and other uses. Figure 2 illustrates the sequence of basalt interbedded with thin sedimentary units that comprise the vadose zone and aquifer (Anderson and Lewis, 1989). Additional scale drawings and other stratigraphic information are in the works of Barraclough et al. (1976), Rightmire and Lewis (1987b), Anderson et al. (1996), Anderson and Liszewski (1997), and Holdren et al. (2002).

Basalts on the eastern Snake River Plain range in age from 3.5×10^6 to 2.0×10^3 yr^{-1}. Near the SDA the basalts are considered in terms of basalt flow groups, commonly about 10 m thick, labeled with letters from A through I (Fig. 2), as discussed below. Three important basalt flow groups, A, B, and C, are within about 70 m of the surface at the SDA.

The sediments include particles from clay to gravel sized. The soil or surficial sediment typically is a few meters thick. Over much of the INEEL it has undergone little artificial disturbance, not having been used other than for grazing animals. Waste burial at the SDA involved removal of some or all soil to the top of basalt flow group A, emplacement of waste, and backfilling of the trench with the excavated soil. The sedimentary interbeds are named AB, BC, CD, etc. after the basalt flow groups they lie between (Fig. 2). Their depths below land surface vary topographically, but the two most prominent interbeds under the SDA, the BC and CD interbeds, are traditionally labeled with depths of 34 and 73 m, respectively.

Sediments

Origin and General Description

Much of the INEEL sediment was deposited by meltwater discharge and periodic floods along the ancestral channel and floodplain of the Big Lost River during past glacial declines (Hughes, 1993; Rathburn, 1993). Another major part of the surficial sediment and sedimentary interbeds is loess and aeolian material derived from fine alluvial deposits having grain sizes ranging from fine silt to very fine sand. Sediments including large amounts of clay-sized material probably were deposited in small lakes, some of which were formed by lava dams. Clay- to sand-sized sediment also was transported by water and wind into the fractures of underlying basalt flows.

Most of the area of the INEEL is within the Big Lost Trough, an area of sediment accumulation along the channel and floodplain of the Big Lost River and between the Big Lost River sinks and Mud Lake (Fig. 1) (Geslin et al., 2002; Gianniny et al., 1997). Sediment within this trough generally grades from a predominance of sand and gravel near the SDA to mainly clay and silt near Mud Lake. Barraclough et al. (1976) hypothesized that the location of the SDA was in the floodplain of the Big Lost River until about 100 000 yrs ago. The presence of gravel in the surficial sediment and interbeds indicates that a watercourse with flow capable of moving gravel-sized grains at least occasionally traversed the area of the SDA during the past few hundred thousand years. Migrations of the Big Lost River probably occurred many times during the geologic past in response to topographic changes produced by basalt eruption.

During periods of volcanic quiescence, sediment accumulated in the topographic depressions of underlying basalt flows to form what are now the sedimentary interbeds. The interbeds closely resemble the surficial sediments in some ways (e.g., mineralogy) and differ significantly in others (e.g., having greater density and more uniform structure). They probably have no significant wormholes or root holes and may be less aggregated than the surficial sediments. Some interbeds are highly stratified; internal layers and lenses can differ substantially in texture, structure, and geochemical composition (e.g., if deposited in different conditions or if baked by a flow of fresh lava).

Two significant periods of loess accumulation in the surficial sediment have been identified: one from about 80 000 to 60 000 yr ago and one from about 40 000 to 10 000 yr ago (Forman et al., 1993). The depositional environment of sedimentary interbed AB has at least two different interpretations. According to Hughes (1993), AB sediment is mainly very fine sand and silt deposited in a floodplain environment. According to McElroy et al. (1989), this sediment is primarily loess. At least one period of loess accumulation in interbed AB, probably about 150 000 to 140 000 yr ago, has been identified (Forman et al., 1993). Hughes (1993) interpreted the sediment of interbed BC as mainly sand and gravel deposited in a braidplain setting in channel systems as wide as 300 m between topographic highs in the basalt. The CD sediment is mainly sand and silt interpreted to have been deposited in low-energy channels and floodplains (Hughes, 1993). The nearly continuous nature of this interbed indicates deposition in a broad, shallow braidplain setting that aggraded to above most of the topographic highs in the basalt (Hughes, 1993). Although interpretations of depositional environments are useful for evaluating overall sediment relations, they are still too generalized to be useful for evaluating the potential for movement of water and wastes.

As determined by sieve analyses, optical scattering, and other methods, grain sizes of surficial and interbed sediments range from clay to pebble sized (Barraclough et al., 1976; Rightmire and Lewis, 1987b; Bartholomay et al., 1989; Davis and Pittman, 1990; Hughes, 1993, Shakofsky, 1995; Perkins and Nimmo, 2000; Perkins, 2003; Winfield, 2003). Most soil and interbed sediment falls within the silt loam textural class, containing about 0 to 27% clay, 55 to 80% silt, and 10 to 35% sand. Fracture- and vesicle-infill sediments generally are finer than interbed sediments because infiltrating water preferentially deposits finer particles in the vesicles and fractures (Rightmire, 1984).

Significant lithologic variations occur within the surficial sediment and sedimentary interbeds as a result of changes in depositional environments through time (Rightmire and Lewis, 1987a, 1987b; Hughes, 1993). Centimeter-scale vertical and horizontal lithologic variations have been investigated for only a few sediment cores. There are discrepancies in the lithologic descriptions by different investigators even for materials from the same boreholes. For example, Rightmire and Lewis (1987a) described the lower part of the CD interbed from one borehole as containing abundant plastic clay, whereas Hughes (1993) described it as sandy silt and slightly silty, fine to coarse sand. Because of these discrepancies and the paucity of detailed descriptions, the role of variations within sedimentary layers in controlling vadose-zone processes cannot yet be fully evaluated.

Weakly developed to well-developed paleosols have been identified in the surficial sediment and sedimentary interbed AB and, although not documented, probably also occur in interbeds BC and CD. Forman et al. (1993) identified paleosols associated with young loess units in two excavations of surficial sediment at the SDA; one of these is thought to represent a prolonged period of pedogenesis, possibly exceeding 20 000 yr. These units contain A, B, and C soil horizons, carbonized zones, and abundant clay cutans having a maximum clay concentration of 36%. Carbonized zones represent vegetation that was inundated and baked by lava flows during the geologic past. Carbonate content of these investigated paleosols, outside of the SDA, generally is smaller than 10% but is as large as 20 to 25% in some zones.

Factors such as sedimentary structures, grain size distributions, bulk mineralogy, clay mineralogy, and ion-exchange capacity influence the movement of contaminants. Sedimentary structures in the surficial sediments, interbeds, or both, include, besides the paleosols noted above, cracks formed by hydrocompaction and desiccation, freeze–thaw features, burrow and rootlet holes, caliche development, horizontal laminations, ripple cross-stratification, planar cross-stratification, lenticular bedding, flaser bedding, rip-up clasts, load casts, and varves (Rightmire and Lewis, 1987b; Hughes, 1993).

Areal Extent, Thickness, and Orientation

In and near the SDA, sedimentary sequences vary in thickness from 0 to 12 m, averaging about 1.5 m. Their thicknesses vary in accordance with the topography of underlying basalt flows. The thicknesses and areal extents of the most continuous interbeds near the SDA (AB, BC, and CD) suggest that these units, like the surficial sediment, accumulated for long enough periods of time to fill and overtop most local topographic depressions. Sediment did not accumulate on some local basalt ridges, and sediment accumulation of interbed AB was restricted in areal extent by the northward-sloping surface of the underlying basalt-flow group, which erupted from a vent south of the SDA, near Big Southern Butte (Fig. 1). Processes like this produced sloping surfaces as well as gaps where interbeds pinch out to zero thickness. Near the SDA the interbeds tend to dip in an easterly direction, the BC interbed about 3.8 m km^{-1} and the CD about 4.7 m km^{-1}, on average (Anderson and Lewis, 1989).

Mineralogy and Chemical Characteristics

Analyses of bulk mineralogy of INEEL sediments show the presence of quartz, plagioclase feldspar, potassium feldspar, pyroxene, olivine, calcite, dolomite, and clay minerals. Bartholomay (1990b, p. 11) statistically summarized the previously published bulk mineralogy data by interbed depth for areas throughout the Big Lost Trough. Additional data are in a report by Reed and Bartholomay (1994). In general, quartz and plagioclase feldspar are the most abundant minerals in the sediment in the south and western portions of the Big Lost Trough, while calcite and quartz are the most abundant minerals to the north. Pyroxene and clay minerals also are present in most of the sediment samples from the INEEL. Dolomite is found in most of the sedimentary samples in the northern part of the basin, but is rarely found in the southern part.

Analyses of the clay minerals sampled throughout the INEEL indicate that illite predominates (ranging from 10–100% of the clay minerals identified), and that lesser amounts of smectite, mixed-layer illite/smectite, kaolinite, and possibly chlorite are present (Bartholomay et al., 1989; Reed and Bartholomay, 1994). The clay minerals that are present in the system provide sites for sorption or ion exchange with any contaminant-bearing water in the system. These processes would inhibit migration of contaminants to the aquifer.

Abundance of clay minerals in interbed samples from the SDA ranges from 0 to 60% and averages about 20% (Bartholomay, 1990b). Olivine is present in some samples in trace amounts. Calcite also was identified in some samples. Rightmire and Lewis (1987b, p. 35–36) reported trace amounts of iron oxyhydroxides, hematite, siderite and dolomite in some samples. Rightmire and Lewis (unpublished data, 1995) reported one tentative identification of the zeolite mineral chabazite. This lack of zeolite in the system probably precludes ion exchange reactions between contaminants in solution and zeolite minerals.

Mineralogical analyses indicate that most of the carbonate in the system is in the form of calcite (Bartholomay et al., 1989). The calcite generally is attributed to the formation of caliche in the interbeds near the SDA (Rightmire and Lewis, 1987b), but is mostly detrital in the northern part of the INEEL. Calcite contents in samples from the SDA range from absent, for most of the samples, to 54%. At the SDA, calcite content larger than 10% was reported for interbeds BC and CD, for surficial sediment, and from a vesicle at about 9 m in a well south of the facility (Fig. 1). The greatest carbonate content in interbed BC is at the base of the interbed (Rightmire and Lewis, 1987b).

Immediately below a basalt flow, interbeds are likely to have a baked zone of sedimentary material whose properties may have been altered by exposure to the heat of fresh lava. Many of the sedimentary interbed materials are dark reddish-brown, which may result from dehydration and oxidation of iron-rich minerals enhanced by heat from the overlying lava flows. This coloration also may result from oxidation of ferrous iron to ferric iron during the weathering of olivine and augite at the time that the interbeds were exposed at the land surface to an oxygenated soil atmosphere (Rightmire and Lewis, 1987b).

Hydraulic Properties of Surficial Sediments

The unsaturated hydraulic conductivity (K) and water retention of the surficial sediments at the INEEL are typical of a soil in which structural features such as aggregation and macropores have evolved over time, as shown by Shakofsky (1995) and Nimmo et al. (1999). Hydraulic and other properties of surficial sediments have also been measured and reported by Barraclough et al. (1976), McElroy and Hubbell (1990), Borghese (1991), and Shakofsky (1995).

At some locations, especially where INEEL facilities have been constructed, soil properties have been substantially altered by mechanical disturbances. Typically such disturbance reduces the effect of large pores and damages or destroys the natural soil horizons and other stratification. These alterations can greatly influence the subsurface hydrology. Although soil disturbed in this

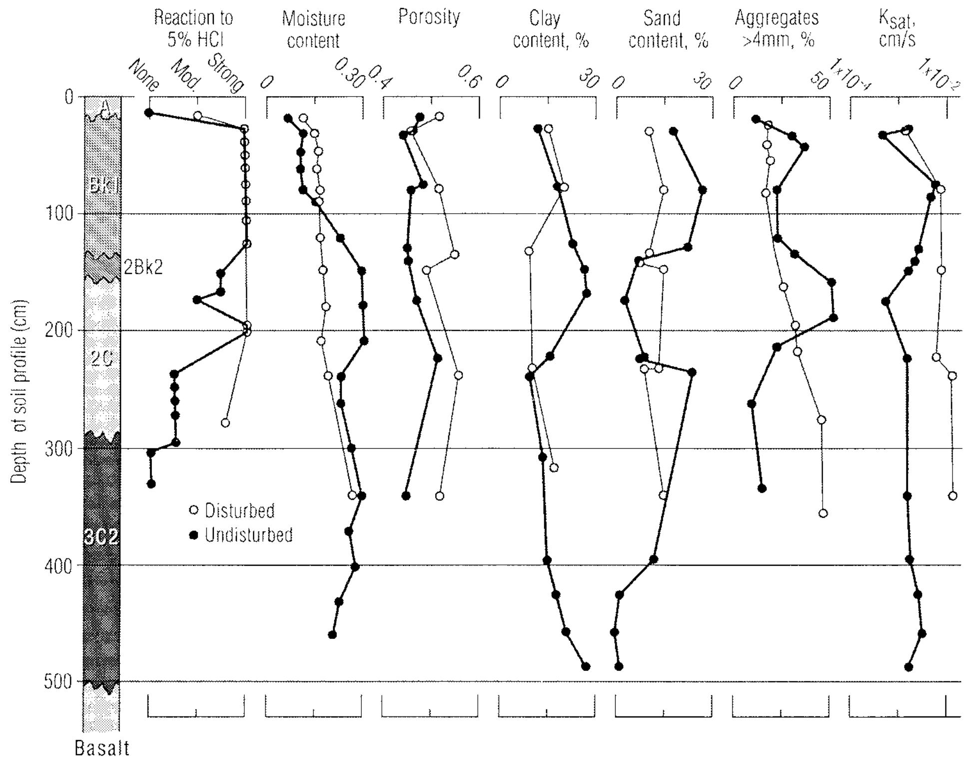

Fig. 3. Depth profiles of selected properties of disturbed soil from a simulated waste trench and of nearby undisturbed soil, at a location adjacent to the INEEL Subsurface Disposal Area (Nimmo et al., 1999).

way occupies only a small fraction of the INEEL, it is important to contaminant hydrology because it surrounds most of the contaminant sources.

Figure 3 gives a basic characterization of selected measured properties of disturbed and undisturbed soil, and illustrates the distinguishable horizons of the undisturbed profile, at a location north of and adjacent to the SDA. Nimmo et al. (1999) and Shakofsky (1995) give additional information about the soil horizons and related data, including particle and aggregate size distributions. Distinct horizon development in the undisturbed profile is clear. The disturbed soil is more homogeneous; the relatively smooth profiles of the aggregate distribution, clay content, and carbonate content portray an absence of natural layers. Probably as a result of this homogeneity, water content in the disturbed profile is also more uniform with depth. Disturbance, in this case construction of a simulated waste trench, has created an essentially unlayered, homogenized soil of unconsolidated sediments with an increased porosity.

Saturated hydraulic conductivity K_{sat} measured on soil core samples varies over six orders of magnitude, from 1.1×10^{-8} cm s^{-1} (Barraclough et al., 1976) to 1.2×10^{-2} cm s^{-1} (Shakofsky and Nimmo, 1996). Although it has not been directly measured, the local anisotropy of hydraulic conductivity may be substantial as it is in general for surface soils with developed structural features.

Measured unsaturated properties reported by Nimmo et al. (1999) characterize both undisturbed and disturbed soil near the SDA. The drying retention curves in Fig. 4 show the air-entry very near zero matric pressure, an abrupt drop to a bend between -10 and -30 kPa, and a nearly flat tail beyond the bend. They differ little between undisturbed and disturbed soils. The shapes are typical of structured surface soils, not of repacked samples. The most obvious disturbance-related distinction is that there is more spread among the undisturbed curves, indicative of layering like most of the results in Fig. 4. There also is more horizontal heterogeneity in the undisturbed soil, evident from the typically greater spread for the paired samples from the same depth, which came from boreholes 2 to 3 m apart. The measured wetting retention curves suggest essentially the same disturbance-related generalizations as the drying curves. For the same samples, unsaturated hydraulic conductivity measurements by several methods show some measurable effect of landfill-construction disturbance. In the undisturbed medium, there is greater spread, indicative of greater heterogeneity, and a tendency toward greater sensitivity of K to water content. The various property measurements imply a broader pore-size distribution for undisturbed soil. It is likely that the excavation and replacement of soil both destroys large pores and breaks up aggregates, reducing the breadth of the pore-size distribution.

Properties of the disturbed surficial soil in the southern portion of the SDA, measured by Borghese (1991), include drying retention curves presented as parameter values of the Brooks and Corey (1964) formula. The curves defined by these values differ from the results of Nimmo et al. (1999) in having air-entry values ranging from -7 to -56 kPa, while those of Nimmo et al. are approximately -0.1 kPa. The measurements of Borghese, however, used a pressure-plate technique that was

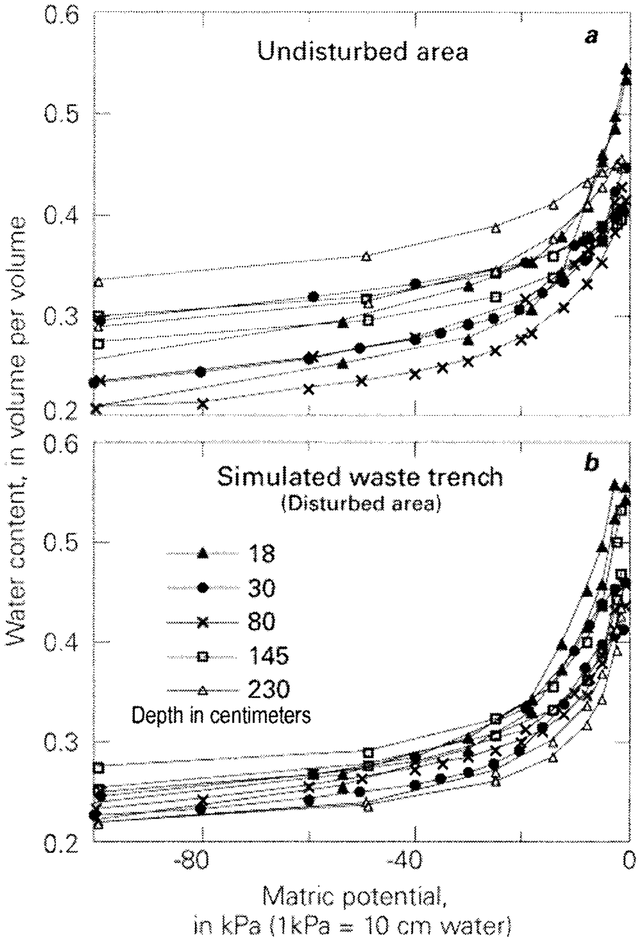

Fig. 4. Water retention curves measured for core samples of disturbed and undisturbed soil from the profiles illustrated in Fig. 3 (Shakofsky, 1995).

insensitive to the range between 0 and −10 kPa, so the more highly negative air-entry values are probably an artifact of the measurement and curve-fitting techniques.

Drying water retention measurements for four samples from the perimeter of the SDA reported by McElroy and Hubbell (1990) fall within or close to the range of measurements in Fig. 4b. The curves show a somewhat more gradual decline in water content (θ) with decreasing matric pressure (ψ), like those of the more water-retentive samples in Fig. 4a.

Hydraulic Properties of Sedimentary Interbeds

The hydraulic properties of interbeds tend to be like those of the surficial sediments except for systematic differences such as smaller wet-range hydraulic conductivity resulting from greater bulk density. Because of their compacted structure with few macropores, interbed sediments are also likely to retain more water after episodes of drainage. Hydraulic properties of interbed sediments have been measured and reported by Barraclough et al. (1976), McElroy and Hubbell (1990), McCarthy and McElroy (1995), Perkins and Nimmo (2000), Leecaster (2002), Perkins (2003), and Winfield (2003) (Table 1). Sampling locations are near the SDA, near the Vadose Zone Research Park (VZRP), and between the VZRP and the Big Lost River as shown in Fig. 1. Many of the samples in these studies contain <50% sand-sized or larger particles, and little or no gravel. Coarse materials are known to exist as a result of high-energy flow events in ancestral channels, although they may be underrepresented in the available data. This underrepresentation may reflect a sampling bias, as finer materials are more easily recovered by the techniques used in the retrieval of deep cores. The coarsest samples analyzed for hydraulic properties contain >90% sand and as much as 7% gravel (Perkins, 2000).

Saturated hydraulic conductivity measured on interbed core samples varies more than three orders of magnitude in interbed AB, more than eight orders of magnitude in BC, and more than seven orders of magnitude in CD (Barraclough et al., 1976; McCarthy and McElroy, 1995; Leecaster, 2002). Leecaster (2002) compiled data for the BC and CD interbeds from various sources and reported a range of vertical hydraulic conductivity of 3.6×10^{-8} to 1.7×10^{-1} cm s^{-1} for the BC interbed and 2.0×10^{-9} to 8.4×10^{-1} cm s^{-1} for the CD interbed. These ranges of hydraulic conductivity probably reflect centimeter-scale changes in lithology, from clay- to gravel-sized clasts, within the sediments. Because the sediments are granular and unconsolidated, the interbeds may be less anisotropic than other parts of the vadose zone.

Perkins and Nimmo (2000) measured a detailed vertical profile of hydraulic properties of the BC interbed at one location near the SDA. At this location, a 5-m-thick layer of silt loam is overlain by 5 m of sand with intermittent gravel lenses that are likely associated with an ancestral channel of the Big Lost River. Figure 5 shows particle size distributions, water retention characteristics, and hydraulic conductivity curves for the two extreme textures at this location. Vertical variation in sediment texture also illustrates the difference in depositional environments over time. Horizontal variability of sediments likely plays a significant role in vertical and horizontal flow behavior. Recent hydraulic property measurements on samples from the vicinity of the Idaho Nuclear Technology and Engineering Center (INTEC) (Perkins, 2003; Winfield, 2003) provide a transect of data that illustrate horizontal variability for one area (Fig. 6). An example based on data from five boreholes is shown in Figure 7. Most of the samples have silt loam texture. Horizontal variability is relatively minimal but is more pronounced in areas traversed by the ancestral Big Lost River. The subsurface is more structurally complex, in terms of number of interbeds and variation in dip angles, near the INTEC than near the SDA, so it is more difficult to correlate interbeds over significant distances. Anderson (1991) identified 23 basalt flow groups and 15 to 20 interbeds in the vicinity of the INTEC.

Basalts

Individual basalt flows mostly are thin (3–9 m), tube-fed pahoehoe flows similar to those of Hawaii (Ander-

Table 1. Studies of surficial and interbed sediment hydraulic properties.

Reference	Nearest INEEL facility	Media	Total samples	Number of measurements: K_{sat}	$K(\theta)$	$\theta(\psi)$	Bulk properties	Particle size
Perkins, 2003	INTEC	Interbed†	14	12	12	14	14	14
Winfield, 2003	INTEC	Interbed†	77	10	10	10	10	77
Leecaster, 2002	SDA	AB, BC, CD interbed	67	44	0	51	51	67
Perkins and Nimmo, 2000	SDA	BC interbed	38	18	18	18	18	38
Nimmo et al., 1999‡	SDA	Surficial	36	32	32	36	0	0
Shakofsky, 1995	SDA	Surficial	24	19	16	20	24	23
Hughes, 1993	SDA	AB, BC, CD interbed	170	0	0	0	0	170
Bishop, 1991	SDA	Basalt	71	29	29	60	71	0
Borghese, 1991	SDA	Surficial	16	14	0	16	14	14
McElroy and Hubbell, 1990	SDA	Surficial, AB, BC, CD interbed	20	20	20	20	20	20
Knutson et al., 1992	SDA	Basalt	25	25	0	0	25	0
Barraclough et al., 1976	SDA	Surficial, AB, BC, CD interbed	46	36	0	0	38	46

† Interbeds near the INTEC are not systematically named as are those near the SDA.
‡ Includes some data from Shakofsky, 1995.

son et al., 1999). They are deposited during individual, brief eruptive events (Kuntz et al., 1980) from numerous fissures and small shield volcanoes on and near the Arco-Big Southern Butte volcanic rift zone (Kuntz et al., 1992). Outcrop exposures indicate that individual basalt flows generally form long, sinuous lobes having median length/width ratios of about 3:1 (Welhan et al., 1997). Some flows are as long as several kilometers (Kuntz et al., 1994). Void spaces in these flows are greatest along their top and bottom surfaces and near volcanic vents. Many of the flows have numerous features such as lava tubes and closely spaced fractures up to a few meters wide and tens of meters long. These may be open or filled with rubble, sediment, or younger lava. In some places, basalt flows are cut by vertical fissures, dikes, and tension cracks associated with northwest-trending volcanic rift zones (Anderson et al., 1999; Hughes et al., 1999). Where they can be observed at the land surface, tension cracks cut vertically through numerous flow groups, are as wide as 2 m, and occur as closely spaced openings along the edges of eruptive fissures over distances of many kilometers.

Basalt flows and other volcanic deposits combine into basalt flow groups, each of which is a complex assemblage of overlapping flows and deposits related to a single eruption. A basalt flow group comprises several, perhaps hundreds, of distinct basalt flows that occurred in a time interval brief enough that little or no sediment accumulated between them.

Basalt rock varies greatly in the degree to which it is fractured. Where fractures are small in aperture and predominantly intercrystalline, the basalt is called dense or massive. At the other extreme, where fractures are so pronounced and abundant that the rock is broken into individual particles, it is called *rubble*, a term which is taken also to include other particulate volcanic material such as scoria. The term *fractured basalt* refers either to the broad middle range of material that is hydraulically dominated by interconnected fractures, or to the basalts as a whole.

Mineralogy and Chemical Characteristics

Most basalt flows at the INEEL have the chemical characteristics of both tholeittic and alkali olivine basalts. These basalts generally are medium to dark gray and range from vesicular, having elongated vesicles up to 4 cm long, to dense.

Typical basalt samples consist mainly of plagioclase feldspar (averaging An_{65}, the composition of labradorite), pyroxene (tentatively identified as augite), and olivine (Fo_{50} to Fo_{90}) and contain lesser amounts of ilmenite, magnetite, hematite, and accessory apatite (Kuntz et al., 1980; Rightmire and Lewis, 1987b; Knobel et al., 1997). Chemical compositions of selected basalt samples at the INEEL were presented in reports by Kuntz and Dalrymple (1979), Knobel et al. (1995, 2001), Reed et al. (1997), and Colello et al. (1998). Stout and Nicholls (1977) stated that the augite contains 18.8% CaO_2 and that opaque minerals constitute between 7 and 21% of the rock. With the exception of some basalt flows at Craters of the Moon (about 2000–18 000 yr old) and basalt flows associated with Cedar Butte (about 420 000 yr old), there are no significant differences in chemical or mineralogical composition related to age or geographic location among basalt flows of the eastern Snake River Plain (Knobel et al., 1997).

Nature of Fractures

In general, the number of fractures and the widths of their apertures are much greater near the top and bottom of a basalt flow and are greatest along the top surface. Knutson et al. (1992) described a range of typical aperture widths measured from outcrops at the INEEL of from 0.0005 to 0.0025 m; however, aperture widths may range from several micrometers to several meters (Rightmire and Lewis, 1987b).

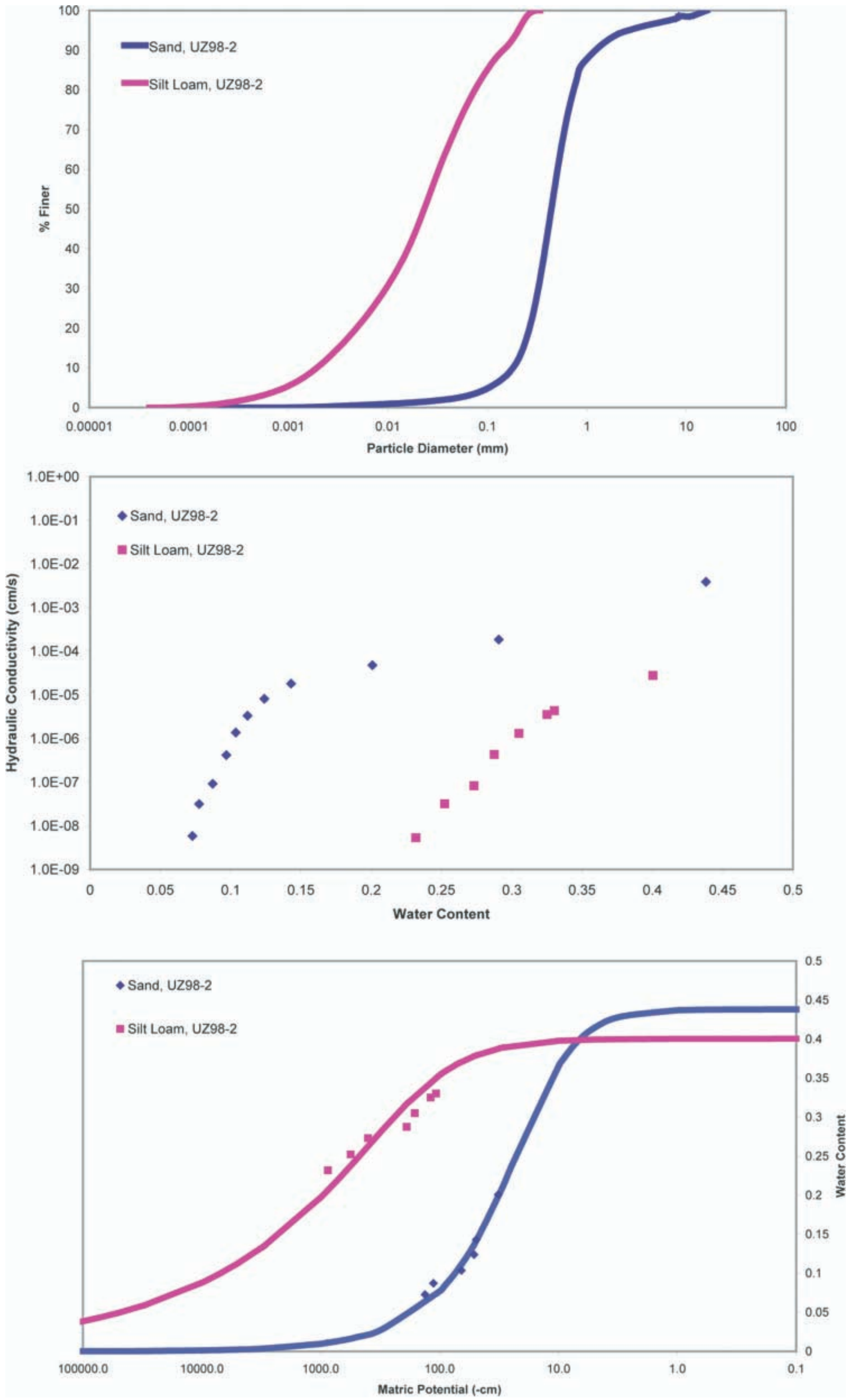

Fig. 5. Measured particle size distribution, water retention curves, and unsaturated hydraulic conductivity of core samples of the BC sedimentary interbed near the INEEL Subsurface Disposal Area. The two samples selected for this illustration are representative of two distinct layers within this interbed, the upper layer of sandy texture and the lower layer of silt loam texture (Perkins and Nimmo, 2000).

Rightmire and Lewis (1987a) described fractures in basalt core samples from the SDA that range from those having fresh surfaces to those containing abundant sediment infill. Fractures having fresh surfaces most likely are dead-end fractures that transmit little, if any, water (Wood and Norrell, 1996; Magnuson and Sondrup,

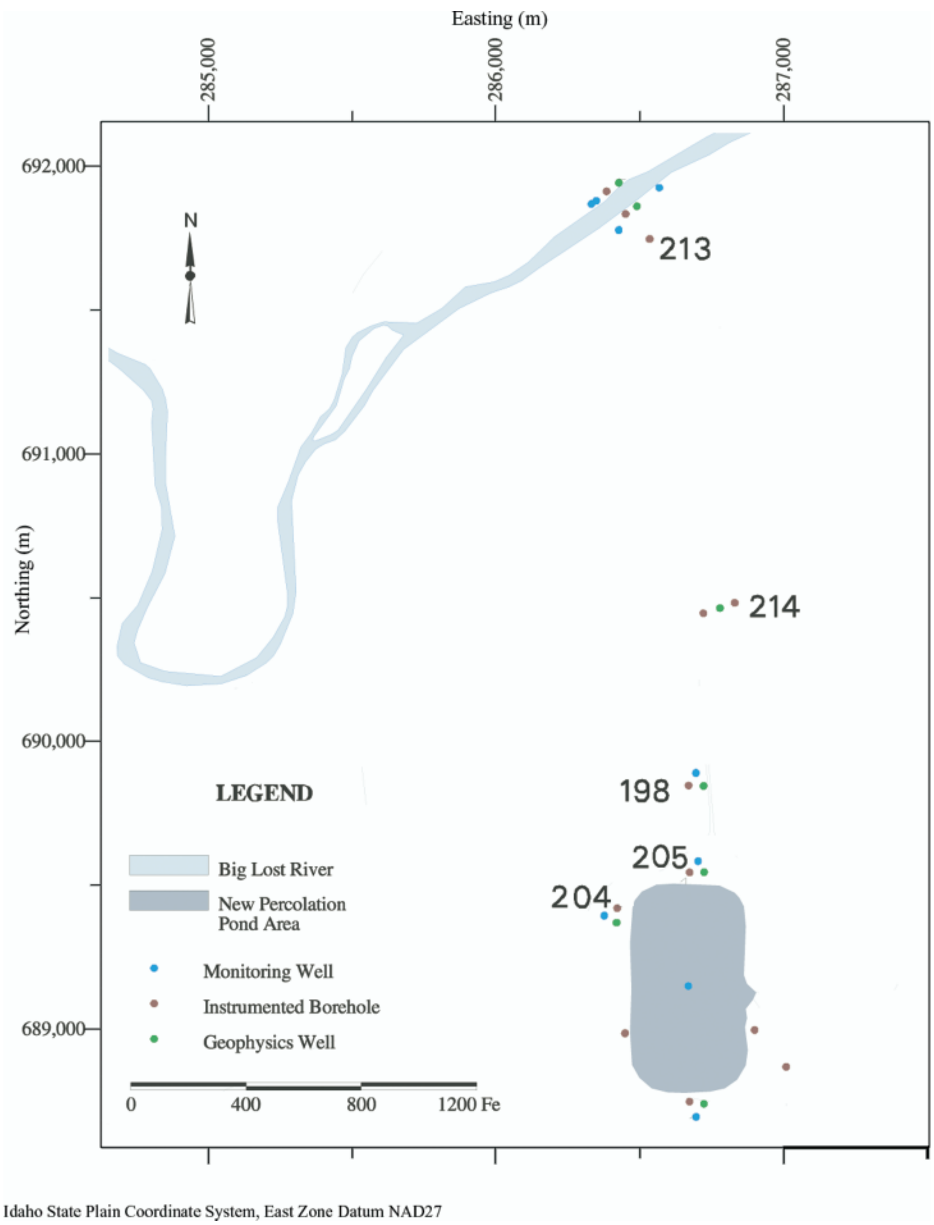

Fig. 6. Locations of holes sampled for investigation of sedimentary interbed properties at the INEEL Vadose Zone Research Park (modified from Bechtel BWXT Idaho, 2002).

1998). Fractures containing sediment infill or coatings probably are interconnected fractures that periodically transmit large quantities of water. Sediment in these fractures ranges from clay to sand sized. Sediment coloration indicates a wide range of minerals and depositional environments and includes hues of tan, brown, red, gray, orange, yellow, and green. Many of the deposits are calcareous. Additional fracture coatings consist of amorphous silica, precipitates consisting of calcite and mixed-layer illite/smectite clays, and, possibly zeolites (Rightmire and Lewis, 1987a).

Fractures and vesicles commonly are coated with fine-grained sediment infill and sometimes with secondary minerals consisting of calcite, clays, and zeolites (Rightmire and Lewis, 1987b; Morse and McCurry, 1997). Fractures within and contacts between individual basalt flows provide a complex network of potential vertical and horizontal pathways for the movement of water and wastes within the vadose zone and the aquifer.

Barraclough et al. (1976) noted that at the contact between basalt and sedimentary layers, the permeable openings into the basalt are partially filled by sediment. Rightmire (1984, p. 32) observed that ". . . sedimentary lining and filling of fractures is the result of water-borne sedimentation. Layers of oriented clay particles overlain by disoriented coarser material suggest a series of minor recharge events followed by a major recharge event to fill the fractures." A layer of basalt in which the fractures are filled with fine sediments may have particularly low hydraulic conductivity.

Rubble

Rubble zones are common along the rapidly cooled margins of basalt flows. Rubble and scoria are widely

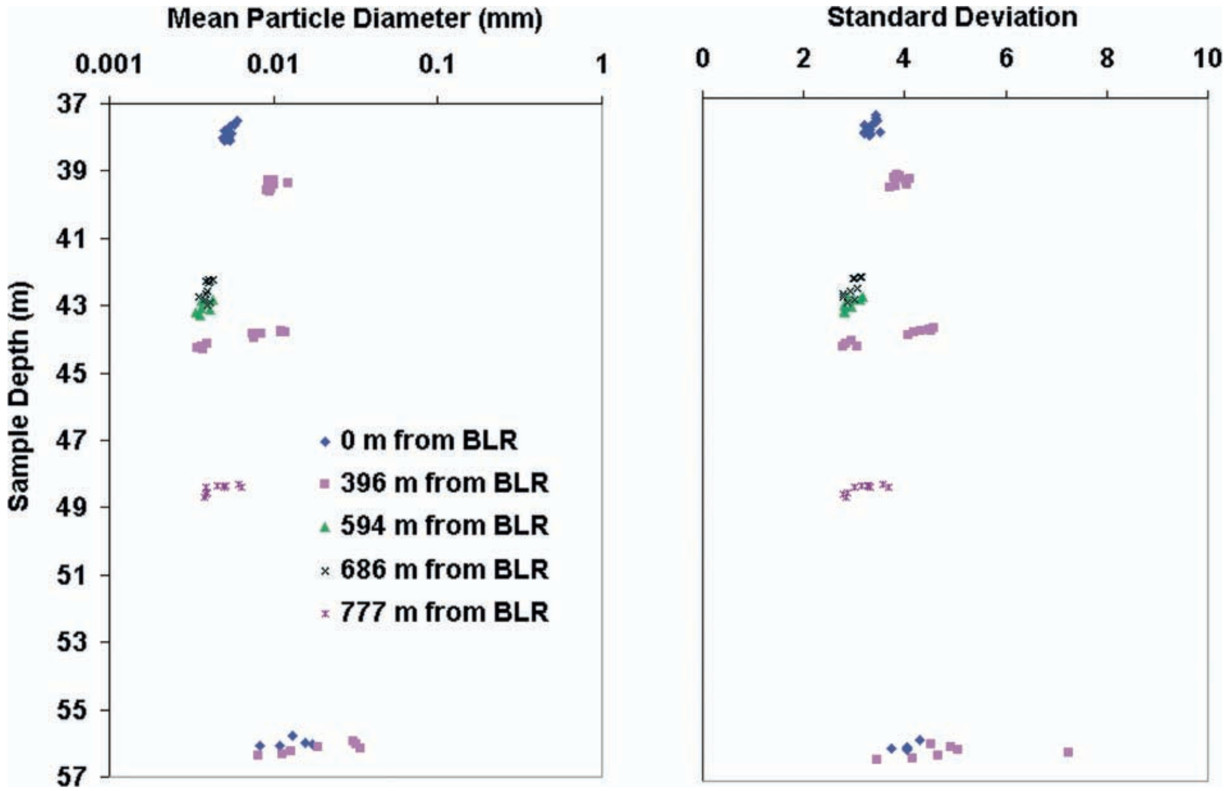

Fig. 7. Texture of interbed sediments near the INEEL Vadose Zone Research Park as mapped in Fig. 6, in terms of the particle-size mean and standard deviation, showing trends with depth and with distance from the Big Lost River (BLR) (Winfield, 2003; Perkins, 2003).

distributed in the vadose zone and aquifer at the INEEL. For example, Magnuson and Sondrup (1998) described a rubble zone across the SDA at a depth of about 60 m.

Smith (2004) described rubble zones as layers of solidified blocks that fall from the front of an advancing lava flow, which then overrides them. Welhan et al. (2002a) described one type as "a highly porous and permeable zone" that is "supported within and on the upper crust of a lobe." According to Welhan et al. (2002a, 2002b), they occur prominently and thickly in the uppermost portion of a lava flow. Geist et al. (2002) said they mostly occur at the upper crust of lava flows. Smith (2004) noted that each basalt flow has a rubble zone at its base. Similarly, but with a different process of formation in mind, Geist et al. (2002) noted that they exist in the scoriaceous lower crusts of some flows. The potential for scoria is greatest near a vent, for example in basalt-flow group C near the SDA (Anderson and Liszewski, 1997).

The thickness of rubble zones is usually about 1 m (Smith, 2004). Welhan et al. (2002b) estimated that the typical thickness is <0.2 m for the rubble itself, and likely from 1 to 1.5 m for rubble plus the most densely fractured upper crust.

Important properties of rubble zones include their porosity, which can be as high as 50% (Smith, 2004). Their hydraulic conductivity is likely to be similar to that of gravel, and could easily exceed 1 cm s^{-1}.

Hydraulic Properties of Basalts

The hydraulic properties of the basalts have been determined using approaches that include single-well aquifer tests, laboratory measurements, large-scale infiltration tests, inverse modeling, and forward modeling.

Based on estimates from single-well aquifer tests of 114 wells at and near the INEEL (Anderson et al., 1999) the saturated hydraulic conductivity of the basalts ranges from about 3.5×10^{-6} to 11.3 cm s^{-1}. It is largest for fractured basalt and near-vent volcanic deposits and smallest for dikes, dense basalt, and altered basalt. About two-thirds of these estimates are >0.03 cm s^{-1}, and about one-third are >0.35 cm s^{-1}. The median is 0.18 cm s^{-1}.

Preliminary results of a subregional steady-state model (USGS MODFLOW 2000) applied to flow in the Snake River Plain aquifer at the INEEL provide large-scale estimates of saturated hydraulic conductivity that range from 0.03 to as high as 3.7 cm s^{-1} (Ackerman, personal communication, 2003). These values represent bulk hydraulic conductivity estimates that effectively minimized differences between simulated and measured heads using four hydrogeologic units to represent the aquifer across an area of 4100 km^2.

The unsaturated hydraulic properties of the fractured basalts have been represented by the effective properties approach (Magnuson and Sondrup, 1998), assuming that the fracture network is equivalent to a high-permeability, low-porosity medium (Becker et al., 1998). Magnuson (1995) determined the anisotropy, fracture porosity, the longitudinal dispersivity, and Brooks and Corey (1964) parameters for unsaturated water retention and hydraulic conductivity by inverse modeling to data collected during the Large Scale Infiltration Test (Dunnivant et al., 1998). These results indicated saturated hydraulic conductivities ranging from 3.0×10^{-4} (vertical) to 9.0×10^{-2} cm s^{-1} (horizontal) using an assumed fracture porosity of 0.05 and a fracture aperture of 0.001 m. Kwicklis compared these results (Rousseau et al., 2004) with a theoretically derived estimate based on the capillary rise equation adapted for apertures of parallel-plate fractures (Kwicklis and Healy, 1993) and concluded that an interconnected fracture density of 34 fractures per cubic meter would result in an effective continuum hydraulic conductivity of 2.8 cm s^{-1}, many times larger than estimates derived from the inverse modeling approach. The large range of these estimates reflects uncertainty inherent from the poorly understood nature of unsaturated flow in fractures, and underlines the difficulty and possible inadequacy of the effective properties approach.

As expected from the basic character of basalt formations, there is substantial large- and small-scale anisotropy in INEEL basalts. Estimated ratios of horizontal/vertical permeability range from about 3:1 to 300:1 (Barraclough et al., 1976; Magnuson, 1995; Magnuson and Sondrup, 1998). The subregional aquifer flow model described previously indicates that this ratio may be as high as 7000:1, based on optimization routines used in the MODFLOW 2000 model to minimize residual heads (Ackerman, personal communication, 2003).

Estimates of the effective porosity of the basalts vary widely with sample location, measurement methods, and sample scale. Void spaces in the basalts are most prominent in interflow zones and their associated rubble, fractures, joints, and vesicles (Hughes et al., 1999, Fig. 12). The effective porosity of fractured basalt generally is greater than that of dense basalt. Estimates of the effective porosity range from 0.05 to 0.25 (Nace et al., 1975; Barraclough et al., 1967; Robertson et al., 1974; Robertson, 1974; Bishop, 1991; Garabedian, 1992; Ackerman, 1995). Large-scale estimates, derived from subregional transient-flow model simulations of the aquifer at the INEEL, indicate effective porosities that range from 0.07 to 0.24 (Ackerman, personal communication, 2003).

DYNAMICS OF VADOSE ZONE FLOW

Components of the Hydraulic System

Surface Conditions

The INEEL receives an average annual precipitation of 221 mm, about 30% falling as snow (Clawson et al., 1989). On average, May and June are the wettest months and July is the driest month (Robertson et al., 1974, p. 8). Seasonal streamflow, snowmelt, and local runoff episodically generate large quantities of infiltrating water for periods of days or weeks. Downward flow from ponded infiltration is likely to be fast and voluminous compared with flow generated only from local precipitation.

The Big Lost River is the principal stream within the INEEL and a major source of recharge to the Snake River Plain aquifer. Robertson (1974, p. 26) noted that recharge from the Big Lost River is the "biggest hydrologic variable" in determining the future behavior of waste constituents in the aquifer. But the Big Lost River has been modified so that its hydrologic influence is not limited to the processes occurring within its channel. To minimize the likelihood of floods at INEEL facilities, a diversion dam was constructed on the river in 1958 and enlarged in 1984. Since 1965, a large proportion of the river's flow has been diverted into a series of four infiltration basins, called spreading areas, which occupy a total area of about 12 km^2 and have an estimated total capacity of 2.8×10^7 m^3. Barraclough et al. (1967) estimated characteristic ponded infiltration rates of 2.5×10^{-6} m s^{-1} (0.22 m d^{-1}) for the first spreading area and 9.1×10^{-6} m s^{-1} (0.79 m d^{-1}) for the second. The average annual flow into the spreading areas from 1965 through 1999 was 4.9×10^7 m^3. In some years (e.g., 1978–1980, 1988–1994, and 2000–2003), no water was diverted. During the wet years of 1982 through 1985 approximately two-thirds of the Big Lost River flow that entered the INEEL was diverted to the spreading areas (Pittman et al., 1988).

The SDA has been flooded in 1962, 1969, and 1982 by local runoff from rapid spring thaws (Holdren et al., 2002). Heavy rainfall and melting snow within the SDA have also introduced water into trenches and pits.

Flow within Surficial Sediments

Local infiltration from rainfall, snowmelt, and runoff initially moves downward. If the infiltration is uniform for a large enough area, it can be treated as one-dimensional vertical flow. Infiltrating water can move quickly down to some depth, perhaps a few centimeters or meters, depending on macropores and soil layers, and then move more slowly. Over most of the INEEL, most of the infiltration eventually exits at the soil surface by evapotranspiration. Water flows and redistributes differently in disturbed and undisturbed soil.

Figure 8 illustrates soil water behavior in response to 24-h flood-infiltration experiments reported by Nimmo et al. (1999). Water-content profiles were measured by the neutron-scattering method in separate, identical experiments in disturbed and undisturbed soil. Figure 8a and 8c show water behavior during the infiltration period for the undisturbed and disturbed soil. In the undisturbed soil, the infiltrating wetting front (Fig. 8a) is diffuse in character. The profile behind the wetting front has a slowly increasing water content. In the disturbed soil (Fig. 8c) the wetting front is sharp, with high and fairly uniform water content behind. In both cases the maximum measured water contents are less than the porosity of the media, as expected because of air trapping during infiltration. A clear distinction is that water initially moves to greater depths faster in the undisturbed soil, for example, reaching about 1.7 m in 6 h while in the disturbed soil it reaches only 0.5 m. This behavior is wholly consistent with the expectation that high-conductance macropores would be common in natural soil but far less abundant in severely disturbed soil. Figure 8b and 8d show redistribution, with the surface covered to suppress additional infiltration and evapotranspiration, during 76 d after the infiltration period.

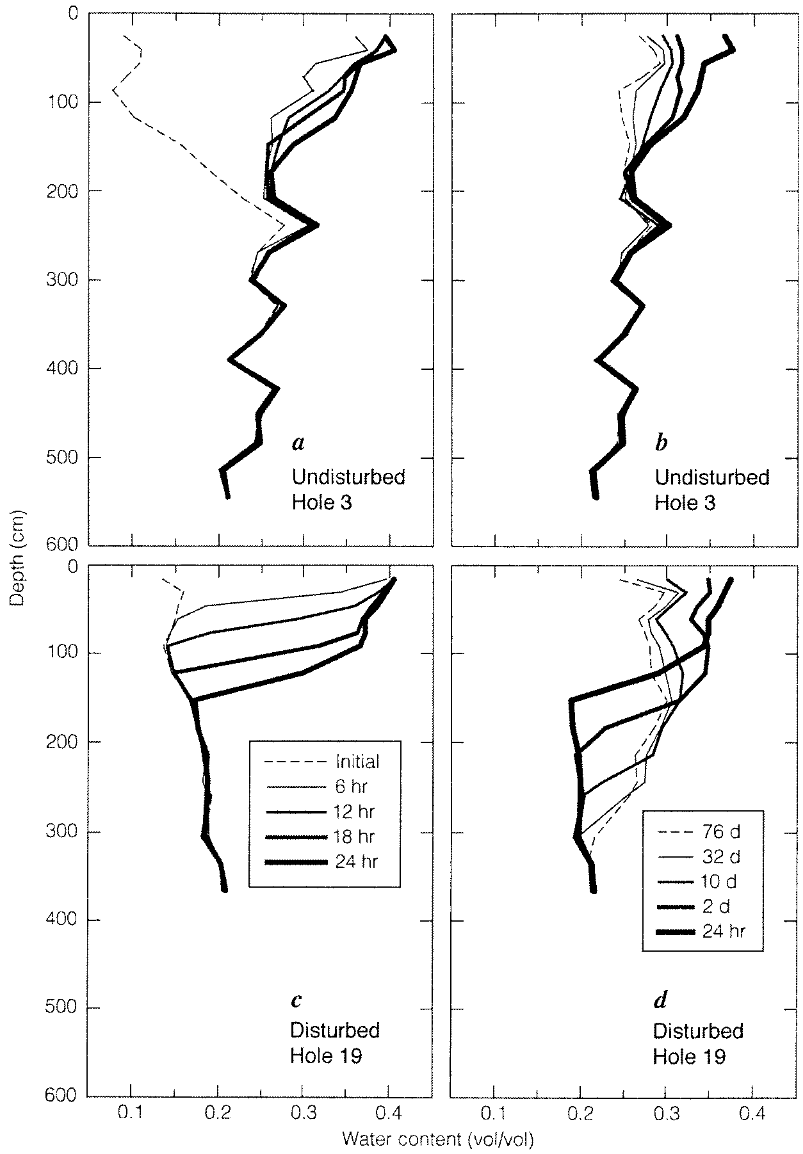

Fig. 8. Water content profiles measured in experiments in (a, b) undisturbed and (c, d) disturbed soil at a location adjacent to the INEEL Subsurface Disposal Area (Nimmo et al., 1999). Profiles in (a) and (c) were measured during ponded infiltration; profiles in (b) and (d) were measured during redistribution with evapotranspiration suppressed.

In the disturbed soil (Fig. 8d) redistribution closely follows the constant-area-rectangle model that frequently applies in homogeneous soils when evaporation is negligible (e.g., Jury et al., 1991). Water appears to move easily and uniformly downwards. It reaches the 3-m depth in about 32 d and shows no evidence of having stopped, even after 76 d. In the undisturbed soil (Fig. 8a and 8b), on the other hand, redistribution does not follow the rectangle model and appears to encounter an impediment to flow at the 2-m depth. In the disturbed but not the undisturbed soil, the infiltrated water appears to remain within the measured profile. In the undisturbed medium, because the soil was covered, the substantial water loss probably does not result from evaporation. More likely it results from horizontal flow that removes water from the range of neutron detection, a process that also could be enhanced by an impeding layer at 2 m. Numerical simulations of this field experiment showed Richards' equation to be consistent with the sharp wetting front and rectangular redistribution in the disturbed soil, but not with the nearly simultaneous wetting within the upper 2 m of the undisturbed soil.

In general, layering and preferential flow should be expected to exert major hydraulic influence in INEEL soil where it is undisturbed. These two elements have opposing effects, layers to retard downward flow, and macropores to increase infiltration by preferential flow when water is applied to the land surface. Even with much preferential flow, flow can be strongly inhibited by an impeding layer. Below such a layer flow is likely to be much steadier. In some cases it is likely to be steady enough that it constitutes a time-averaged flow representing the net effect of variable or episodic flow from above the impeding layer. In such cases it indicates a long-term average rate of deep percolation (the rate of water moving below the root zone) as discussed below in the section on recharge.

Where the soil has been disturbed by such operations as excavation and replacement, the destruction of layers and macropores has significant hydrologic influence. Water moves relatively freely and uniformly to deeper depths. Although the Nimmo et al. (1999) experiments showed no apparent depth limit to the vulnerability of disturbed soil to significant water content increase, the effects of the 24-h flood were significantly attenuated over the days required for water to reach depths exceeding 2 m. Normally, evaporation would not be suppressed, so the increase at these depths would be even less. Although disturbance destroys layers and macropores, which have opposing hydraulic effects, the disturbance may have the net effect of increasing deep percolation because of the loss of impeding layers that otherwise would act to hold water close enough to the land surface for removal by evapotranspiration.

Flow within Sedimentary Interbeds

Flow behavior in sedimentary interbeds varies widely both seasonally and sporadically as water content and hydraulic conductivity vary. At least to some degree, sedimentary interbeds are likely to impede vertical flow and to cause preferential flow from basalt fractures to become more diffuse. The observed perching of water in and above interbeds supports this.

The interbeds probably have less macropore flow within them than the surficial sediments or basalts, but their layered structure may be conducive to funneled or unstable flow (discussed further below under Flow in the Integrated Vadose Zone). Laboratory measurements show that layers of particularly low hydraulic conductivity commonly exist within interbeds, often near sediment basalt contacts (Barraclough et al., 1976; Perkins and Nimmo, 2000; Perkins, 2003), and that saturated hydraulic conductivity can vary by several orders of magnitude within an interbed. Thus, it is likely that, to some degree, they cause vertical and horizontal preferential flow. If fast pathways are common and operative to a significant degree within interbeds, they would significantly influence contaminant transport, such as by lessening adsorptive processes.

Whether the interbeds on the whole act more as barriers to downward flow or as zones of substantial preferential flow is not yet clearly known. Compared with the surficial sediments, there is much less direct evidence concerning flow behavior in the interbeds, mainly because it is difficult to investigate by field experiments that isolate the effects of interbeds from the system as a whole. Depending on the magnitude and prevalence of critical hydraulic processes within these layers, they may retard or accelerate contaminant transport, dilute or fail to dilute contaminants, and establish the dominant movement as vertical or horizontal.

Flow within Basalts

Flow within the basalts is dominated by macropore flow through fractures; the basalt matrix is sometimes assumed impermeable, which for many purposes is likely an adequate approximation. A large body of evidence, including that of the Large-Scale Infiltration Test (Dunnivant et al., 1998), indicates that when the basalt fractures are filled, they can conduct rapidly, perhaps meters per day or faster. Some fractures become filled from wetting events that might occur as often as once or more per year. There is also evidence that some fractures, especially ones with dead ends, do not conduct significant flow, or at least do not allow significant downward flow (Dunnivant et al., 1998). Little is known about the processes or rates of flow in parts of basalt in which all fractures are unsaturated. A common assumption, possibly valid for some purposes, is that such flow is negligible compared with episodic flow through filled macropores.

Flow within Rubble Zones

Flow in rubble zones appears essential to explain the fast, long-range, horizontal vadose zone flow which is increasingly confirmed by observational evidence, such as the field tracer experiments of Nimmo et al. (2002).

That rubble zones can conduct large water fluxes horizontally when wet is established in one way through their effect within the aquifer. The great horizontal hydraulic conductivity of the Snake River Plain aquifer has been credited to what are termed *interflow zones*. Welhan et al. (2002a) described a Type I interflow zone as a combination of highly porous and permeable upper crust and rubble that is commonly observed on lava lobe surfaces. This type of structure, in whole or in part, is a rubble zone. A Type II interflow zone, according to Welhan et al., is a network of tension fractures in inflated pahoehoe, and thus would not normally consist of rubble.

Because vadose zone perching in response to unusually intense infiltration commonly occurs in basalt as well as sedimentary layers, there is a clear possibility for rubble zones to become effectively saturated from time to time, and so to constitute an extremely conductive layer. Some of the rubble-zone formation mechanisms (e.g., development along individual lobes of basalt; Welhan, 2002b, Fig. 2) would not likely create a conductive zone that exists over distances of 1 km and more. Thus the large-scale tracer evidence of Nimmo et al. (2002) supports the possibility of rubble-zone formation mechanisms with large-scale continuity (e.g., rubble forming the base of all basalt flows) under at least some circumstances.

Flow in the Integrated Vadose Zone

Different modes of flow, which may be organized into the two broad categories of diffuse flow (quantifiable with Darcy's Law and Richards' equation) and preferential flow (more narrowly focused and usually faster than diffuse flow) occur within the INEEL vadose zone.

If diffuse flow were the only category of significance, transport in the vadose zone would proceed according to traditional assumptions that it is slow (a few meters per year or less) and predominantly vertical. Slow transport results from typically low values of unsaturated hydraulic conductivity. Vertical transport is likely if the main transport mechanisms are dominated by gravity, as opposed to pressure or concentration gradients, and if the subsurface is effectively homogeneous within each horizontal plane. These generalizations are likely to be applicable some or all of the time in some portions of the geologically diverse INEEL vadose zone, for example where soil has been artificially homogenized, as described above.

Preferential flow transports water and contaminants horizontally to adjacent regions or vertically to the aquifer far sooner than might be predicted based on bulk medium properties and Richards' equation. Another important effect of preferential flow is that a relatively small fraction of the subsurface medium interacts with the contaminants, which limits adsorption and other attenuating processes. Three basic types of preferential flow are macropore, funneled, and unstable (or fingered) flow. Macropore flow has been mentioned above in terms of large soil pores and fractures in basalt. Funneled flow occurs in connection with contrasting layers or lenses, where flow deflected in direction causes a local increase in water content and therefore in hydraulic conductivity and flux. Unstable flow most commonly occurs where water enters a contrasting layer and local instabilities on the plane of contact generate fingers of high water content and flux. It may persist within that layer for several weeks or more. Unstable flow has at least two complications that do not apply to macropore or funneled flow. First, it is not tied to particular permanent features of the medium. Second, the preferentiality of unstable flow changes dynamically, for example by growth in finger width as flow progresses. Theories of unstable flow in terms of scaling and other concepts have been developed by Raats (1973), Parlange and Hillel (1976), Glass et al. (1989), and Hendrickx and Yao (1996).

Information on the particular rate, direction, and mode of flow in the INEEL vadose zone comes from diverse sources, that relate to this problem with varying degrees of directness. Tracers in the form of solutes or pulses of water fairly directly indicate flow rate and direction (e.g., Dunnivant et al., 1998; Nimmo et al., 2002). Often the tracers used in such studies preexist in the environment from natural or artificial causes (e.g., Cecil et al., 1992; Busenberg et al., 2001; 1993). Measurements of water content and matric pressure with time (e.g., Davis and Pittman, 1990; Pittman, 1989; Pittman, 1995; Perkins, 2000; and McElroy and Hubbell, 2003) provide data for calculation of fluxes, and through changes with time may indicate fluxes directly. The dynamics of variably saturated conditions (e.g., perching, mounding of water on the aquifer, fluctuation of measured water levels) can suggest vadose zone flow rates and directions (e.g., Orr, 1999).

Processes of Vertical Flow

In the general case of a stratified vadose zone, contacts between layers that contrast in hydraulic properties (whether obvious rock–sediment contacts or subtler textural contrasts within sediments or within porous rock) impede vertical flow by various mechanisms. When water moves down from a coarse to a fine layer, as from coarse sand to silt, if both layers are near saturation, the fine layer has smaller hydraulic conductivity. Therefore, flow slows when it reaches the fine layer. If the coarse layer is nearly saturated, but the fine layer is initially fairly dry, it is possible for flow to be initially dominated by the sorptive nature of the fine medium, which acts to suck water out of the coarse material. In the latter case the fine layer does not impede flow until more uniformly saturated conditions occur. Where a fine layer overlies a coarse layer, water moving downward is impeded under many conditions. When coarse material is dry, it has an extremely small hydraulic conductivity; thus it tends not to admit water into the pores and exhibits a somewhat self-perpetuating resistance to flow. Water breaks into the coarse layer if the pressure at the layer contact builds to the point that the water-entry pressure (the minimum water pressure needed to fill an empty pore) of some of the large pores is exceeded. This can generate instabilities, as discussed above. Stable or not, water flowing into the pores of the coarse medium drastically increases its hydraulic conductivity. Stable flow through layers where fine overlies coarse is slower than it would be if both layers had the properties of the fine medium. Miller and Gardner (1962) demonstrated this effect experimentally. Thus, the boundaries between any adjacent layers (e.g., sandy and silty layers within interbeds) may retard flow under unsaturated conditions.

A thin surficial layer of small hydraulic conductivity, like the soil at the INEEL, can limit downward flow to the point of being the dominant influence on flow through the sequence. Stothoff (1997) considered a granular medium above fractured bedrock, similar to much of the INEEL vadose zone. The bedrock admits water only under nearly saturated conditions. Stothoff's interpretation assumes the fractures are of greater-than-microscopic width and the rock is otherwise impermeable. The thickness of the granular layer strongly influences the fraction of average precipitation that flows into the bedrock (and presumably further, to the aquifer); a thin alluvial layer more easily becomes saturated to the layer contact and hence more frequently permits deep percolation.

Once water moves through the surficial sediment, or directly into basalt where sediment is absent, vertical water movement through the vadose zone is largely controlled by fractures in the basalt and by the smaller hydraulic conductivity of the interbed sediments. The travel time from the land surface to the top of the first basalt layer may range from a few days to a few years. Travel time through a saturated fractured basalt layer tens of meters thick could be from days to weeks (Dunnivant et al., 1998; Nimmo et al., 2002), while flow through unsaturated fractures is likely to be slower (Tokunaga and Wan, 1997; Su et al., 1999).

When downward flow through basalt fractures reaches the top of a sedimentary interbed, the flow can move in various ways. This flow, like flow through the surficial layers, can be a combination of diffuse and preferential flow. It is probably slower than flow through fractured basalt. Because interbed characteristics are different from those of the surficial sediment and because evapotranspiration at a basalt–interbed contact is insignificant, the flow at these contacts in some ways differs markedly from flow through the surficial sediment.

At the bottom of a sedimentary layer, at the contact with the basalt, water accumulates until the sediment is wet enough to allow breakthrough into one or more fractures, or until the wetted portion of the contact broadens enough to include the entrance to a fracture that is already an active downward conduit. Sometimes this accumulation causes perching just above the basalt contact (Bishop, 1996). Another flow-inhibiting process at the base of a sedimentary layer may result from the lower porosity of the basalt and the distances between its fractures. Barraclough et al. (1976) described this process, noting, "At the contact, perhaps only 10% of the basalt surface is composed of permeable openings, and these are partially filled by sediment. The other 90% is virtually impermeable. This, in effect, provides a thin skin that is estimated to have one-tenth or less of the permeability of the sediments alone." That water commonly perches in and near interbeds suggests that, in at least some circumstances, the interbeds conduct downward flow much more slowly than the basalts.

Recharge

Some fraction of infiltration becomes deep percolation, which is likely to become aquifer recharge. The depth that water must reach for virtual certainty that it will continue downward may be the depth to the fractured basalt, or it may be approximated as the maximum depth at which plant roots are active. At most locations in the INEEL, this depth is a few meters. In the disturbed area of the SDA, where grasses are the dominant vegetation, the depth of active roots is about 2 m.

Diffuse areal recharge, that is, recharge that derives from immediate infiltration of rainfall and snowmelt without collection into surface-water bodies, on the eastern Snake River Plain generally is expected to be small. For an estimated average rate of downward flow, if it is gravity-driven below a certain depth, K at the field water content of that depth can indicate the downward flux density (Nimmo et al., 1994). If water content is essentially constant at a depth of a few meters, at about 0.23 m in the undisturbed and 0.20 m in the disturbed soil, then the K results of Nimmo et al. (1999) with the assumption of gravity-driven flow, indicate about 1 mm or less of deep drainage per year. This is the same order of magnitude as the estimates of 3.6 to 11 mm yr^{-1} that Cecil et al. (1992) obtained by tracer and Darcy-based methods. Assuming there are no losses of water between 3 m and the water table, the range of estimates from these two studies would directly represent recharge rates. Assuming an average water content of about 0.2, the corresponding rates of convective transport would be 5 to 50 mm yr^{-1}. Estimates of this magnitude do not explain the findings of contamination at considerable depths (Humphrey et al., 1982; Laney et al., 1988), suggesting that there are operative flow modes outside of those assumed in this analysis, or significant recharge that does not fall in this category.

Topographically focused recharge may occur from major surface-water features as discussed above, and also from local runoff accumulating in low-lying areas. The SDA, for example, is in a topographic depression. Rapid infiltration of ponded surface water causes recharge that locally affects water levels in the Snake River Plain aquifer. Pittman et al. (1988) observed that the water table in the vicinity of the SDA rose as much as 4.9 m during 1982 through 1985 in response to recharge from surface water diverted to the spreading areas. The rapid downward convective transport (exceeding 20 m d^{-1}) reported by Nimmo et al. (2002) also underlines the importance of this type of recharge.

Perching

Perching, an accumulation of water in a region of the vadose zone such that it becomes locally saturated even though there is unsaturated material below, commonly occurs at the INEEL. It usually results from a large flux of water that encounters a severely impeding layer. It may be a temporary or permanent feature, depending on the nature of the medium, the prevailing hydrologic conditions, and the effect of artificial modifications, as discussed above in terms of the processes of vertical flow. In most cases perched zones are temporary, persisting until horizontal and vertical flow spreads them out enough to leave the porous materials unsaturated.

Several studies (Barraclough et al., 1976; Rightmire and Lewis, 1987b; Anderson and Lewis, 1989) have shown that water episodically accumulates in perched layers that typically persist for a few months. Perched zones commonly extend horizontally for hundreds or thousands of meters. The artificial infiltration of wastewater has created perched zones that have persisted for several years (Orr, 1999). Barraclough et al. (1976, p. 51) noted the presence of perched water in several boreholes within the SDA. They observed that an extensive zone of saturated to nearly saturated basalt existed beneath the SDA. The source of water was not known, but they believed that thin perched-water zones could represent long-term local accumulation of percolating precipitation or more recent accumulation from the 1969 flood at the SDA. The tracer experiment of Nimmo et al. (2002) showed that substantial perching of water under the SDA and elsewhere results from the percolation of water from the spreading areas. Cecil et al. (1991) analyzed water levels in wells and measured water content profiles, showing that perching can take place within both sediments and basalts, and suggested that specific layer contrasts that cause perching at the INEEL might include contacts between (i) basalt flows and sedimentary interbeds; (ii) basalt flows and baked zones; (iii) fractured basalt and dense, unfractured basalt; and (iv) fractured basalt with and without sediments or authigenic mineral deposits filling the fractures.

Perching complicates a contamination problem in several ways. The high water content of a perched zone causes greater hydraulic conductivity and potentially faster transport through the three-dimensional system. The main effect is not a direct increase in vertical flux because the increase in effective vertical hydraulic conductivity is offset by a diminished vertical hydraulic gradient within the perched water. (Vertical flux within and below the perched water cannot be faster than the vertical flux above the perched water or the perched water would have drained). Horizontally, however, there may be greatly increased flow. New and different processes may significantly affect contaminant transport in a perched zone. Reduced aeration, for example, may affect biochemical processes. At the scale of the entire stratified vadose zone, perching may significantly increase anisotropy. Horizontally for considerable distances the hydraulic conductivity might be 1 cm s^{-1} or so, as for a saturated gravel. At the same time, however, vertical flow might be limited by an unsaturated layer having vertical hydraulic conductivity ten or more orders of magnitude less, as for basalt without water in its fractures.

Horizontal Flow

Water movement in the INEEL vadose zone may be predominantly vertical, but it is significantly retarded and diverted by features of the basalts and sediments. Horizontal water movement through the basalt–sediment sequence is largely controlled by the great conductances of basalt fractures and rubble. In the saturated zone, these features provide the main conduits for groundwater flow. In the vadose zone they have the potential to channel perched water over large distances within short periods of time. Fast horizontal flow generally requires an impeding layer below the zone of horizontal flow, as the situation is essentially a case of funneled flow, as explained above. Rapid, high-volume infiltration is likely to greatly enhance the magnitude of vadose zone horizontal flow.

A variety of evidence demonstrates horizontal vadose zone flow and its possibilities. At a modest scale, Rightmire and Lewis (1987a) found grout cement below the BC level in a well for which the nearest likely source of such material was a well 168 m away, the likely pathway being a rubble zone beneath the BC interbed. Nimmo et al. (2002) reported tracer evidence of horizontal flow rates $>$14 m d^{-1} and extending for more than 1 km in the vadose zone in or above both the BC and CD interbeds. The pattern of detections and nondetections in sampled perched-water wells showed the horizontal spreading was not uniform with direction. This essentially confirmed the hypothesis of Rightmire and Lewis (1987b, p. 83), who noted anomalously light isotopic content in water samples from perched water samples at the SDA, indicative of a water source at an altitude higher than the surface of the Snake River Plain, as evidence for accumulation of water as a perched mound on the CD interbed which moves horizontally to the SDA from the location of the Big Lost River or spreading areas. For this to occur as rapidly as observed in the tracer experiment of Nimmo et al. (2002), it is likely that the interbeds caused perching that extended upward into some portion of the overlying basalt. Tracer found under the SDA was in the CD interbed, while tracer found by Nimmo et al. at a comparable distance at the site of the Large Scale Infiltration Test (Wood and Norrell, 1996) was in the BC interbed. In both cases this is consistent with the average dip of these interbeds with respect to particular areas of tracer application.

Horizontal transport for longer distances is also possible. Anderson and Lewis (1989, p. 20) noted that the potential for horizontal flow away from the SDA along the east-sloping surface of the CD interbed is large, highlighting as relevant features the distribution and characterization of flow contacts, fractures, and vesicles, and the lithology of major sedimentary interbeds.

Water moving horizontally is likely to migrate toward depressions at sediment–basalt contacts. Anderson and Lewis (1989, p. 38 and 47) described the sediment–basalt contact on the top of basalt-flow group C in the western part of the SDA as having interbed thickness changing abruptly from 0 on a basalt ridge to more than 6 m in an adjacent depression. Rightmire and Lewis (1987a) suggested, on the basis of carbonate encapsulating clay pellets covered with desiccation cracks present in interbed BC, that sediment and water collected in a topographic depression at the present-day location of Wells 76-4 and 76-4A during the deposition of interbed BC.

Observed rapid horizontal transport could occur through interconnected rubble zones, tension cracks, or similar features if they are nearly saturated. An additional requirement is that there be substantial impediments to vertical flow, such as interbeds or dense basalt that cause perching that extends upward into the highly conductive layer or flow path. Such horizontal movement of water for distances of a kilometer or more suggests that primarily the largest features of basalt flows, flow groups, and volcanic rift zones are most active in this.

Combined Vertical and Horizontal Flow

Because of the great anisotropy of the INEEL vadose zone, vertical-flow impeding features coincide with horizontal-flow promoting features. This means that with even minor inhomogeneities, such as a slight local dip in a sedimentary layer, horizontal flow can be easily generated from the generally expected downward flow. This effect is more pronounced in the presence of perched water. A given observation of perching may result not necessarily from local infiltration but from water that has moved horizontally from a wetter area. Rapid, high-volume vertical transport, as from ponded infiltration, can cause rapid, high-volume horizontal transport.

Even though impediments to vertical flow are effective in causing substantial perching and horizontal diversion, they are not perfect barriers. Results of Nimmo et al. (2002) showing tracer in aquifer samples 9 d after it was applied in the spreading areas show that at least under ponded infiltration, fine-textured interbeds and layers of particularly dense basalt do not prevent the rapid, high-volume, vertical flow that is expected through fractured basalt.

Another process that may be common is funneling. Horizontal flow, especially when enhanced by perching, may bring much water to points where the vertical conductivity is locally large (e.g., where there is a vertical fracture) or to where perching occurs at a sloping contact along which the enhanced flow has a significant vertical component. Water in perched layers could thus entrain contaminants and move them horizontally to places where vertical travel times are less than they are at the source of contamination. By this mechanism additional water added to the system 1 km or further away may reduce vertical travel times to less than they would be for only locally generated flow. Where perched zones are large in horizontal extent, these effects related to horizontal flow can be as important or more important to contaminant transport than is vertical flow.

CONTAMINANT TRANSPORT

Sources

Vadose zone contamination at the INEEL derives mostly from disposal of solid waste, especially at the SDA, although some is also present from such sources as fallout of airborne contaminants and wastewater disposal at the land surface. Radioactive waste has been buried at the SDA since 1952. Until 1970, low-level and transuranic radioactive wastes were buried in pits and trenches. Wastes sometimes were dumped randomly into the pits and compacted, which could have damaged containers. Since 1970, burial of low-level radioactive waste has continued and transuranic waste has been stored on above-ground asphalt pads in retrievable containers. Between 1952 and 1997, approximately 215 000 m^3 of low-level and transuranic waste containing about 12.6 million Ci of radioactivity was buried at the SDA (French and Taylor, 1998, p. INEEL-3). About 0.3 million Ci was attributed to transuranic radioisotopes, according to the inventory of Holdren et al. (2002, Tables 4–1 and 4–2), which includes the annual amounts buried of 25 radioactive and 4 nonradioactive contaminants.

The waste buried at the SDA is in a variety of different physical forms that include containerized sludge, assorted solid wastes, empty contaminated drums, sewage sludge, nitrate salts, depleted uranium waste, and secondary sources such as contaminated asphalt and soil (Humphrey et al., 1982; Becker et al., 1998, p. 3-38–3-42). The waste is packaged in a variety of containers, such as steel boxes, concrete casks, steel drums, plywood boxes, cardboard boxes, and other containers (Becker et al., 1998, p. 6-2). Breaching of these containers or diffusion of contaminants through the container walls allows contaminant release. Although this process does not precisely follow the definition of point source contamination, the nonsystematic release of contaminants in a small area and the release by historic waste disposal methods combine to produce many individual point sources of diverse contaminants in close proximity.

The chemical forms of the buried waste are diverse and not completely known. For example, Navratil (personal communication, 1996) indicated that the major Pu residue processes at Rocky Flats, Colorado from which much of the actinide waste originated, consisted of dissolution, ion exchange, precipitation, fluorination, and reduction. Plutonium tetrafluoride (PuF_4), a finely divided powder, was involved in the last two processes. Because the powdered PuF_4 easily contaminates items such as plastics, paper, gloves, and filters, it is reasonable to conclude that waste buried at the SDA contained Pu in the form PuF_4. Other forms of Pu also are buried at the SDA.

Concentrations of contaminants that slightly exceed the essentially zero background concentrations (Knobel et al., 1992) have been detected in surficial sediments near the SDA (Markham, 1978; Beasley et al., 1998a, 1998b). For example, the range of $^{239+240}$Pu concentrations near the SDA, expressed as total subsurface radioactivity per land surface area, is from about 50 pCi m^{-2} to greater than 600 pCi m^{-2}; however, concentrations in 11 of 19 samples ranged from 270 to 650 pCi m^{-2} (Beasley et al., 1998a, Fig. 15). These contaminants in the shallow subsurface are a potential source of contamination to the vadose zone and ultimately to the eastern Snake River Plain aquifer. The concentrations of these contaminants at the SDA are sufficiently large to be measured with conventional methods, but at distances of more than about 2 km from the SDA, mass spectrometry would be required to detect the concentrations (L.D. Cecil, personal communication, 1999). In the layered vadose zone beneath the SDA, these contaminants could be transported by a variety of natural preferential flow processes as discussed in previous sections. Chemical, biological, or physical means of mobilizing or retarding contaminants could affect contaminant migration. One implication of the widespread distribution of slightly larger than background concentrations of contaminants in surficial sediments is that extreme care should be exercised during drilling operations to avoid dragging contaminants into the deeper subsurface.

Water Chemistry and Contaminant Mobility

Several chemical conditions of water affect the mobility of contaminants. Water from perched zones below the SDA and from the Snake River Plain aquifer has the following characteristics that can significantly affect contaminant transport: (i) pH that ranges from 7.8 to 8.4, (ii) dissolved O_2 concentrations that are nearly saturated to slightly supersaturated with respect to air, (iii) saturation indices that indicate the water is typically nearly saturated with respect to calcite, and (iv) dissolved organic C (DOC) concentrations that are generally smaller than 1 mg L^{-1} (Knobel et al., 1992) or about 1 mg L^{-1} (Busenberg et al., 2000). Generally, larger DOC concentrations are in water from wells that are contaminated by drilling-fluid surfactants or show evidence of other anthropogenic organic contamination (Busenberg et al., 2001). In a previous study (Leenheer and Bagby, 1982) significantly larger DOC concentrations, from 1.6 to 18 mg L^{-1}, were measured in INEEL groundwaters.

Water-chemistry data from the Big Lost River at Arco, ID, upgradient from the SDA (Rightmire and Lewis, 1987b; Bartholomay, 1990a), indicate that the surface water is a calcium bicarbonate type that includes small amounts of Mg and SO_4^{2-}.

Water-chemistry data for perched groundwater at the SDA vary depending on the location of the wells and the timing of sample collection. Perched water at the SDA is attributed to local infiltration of snowmelt and rainfall and to recharge from the Big Lost River and the INEEL spreading areas; some samples contain waste constituents leached from radiochemical and organic wastes (Bartholomay and Tucker, 2000). Samples collected after wells were drilled often show evidence of reactions with cement used in well completion (Rightmire and Lewis, 1987b). Water-chemistry data for perched groundwater above the CD interbed were presented by Barraclough et al. (1976), Rightmire and Lewis (1987b), Hubbell (1990), Knobel et al. (1992), Tucker and Orr (1998), Bartholomay (1998), and Bartholomay and Tucker (2000). These data were mostly collected from Well USGS 92, which has been influenced by spreading area recharge (Nimmo et al., 2002) and shows chemical characteristics similar to Snake River Plain aquifer water (Rightmire and Lewis, 1987b). Rawson et al. (1991) and Rawson and Hubbell (1989, p. 245) determined major ion concentrations of soil pore-water samples. Water in the shallow boreholes was either a sodium chloride or sodium bicarbonate type, and water in the deeper boreholes was a sodium chloride type.

Water samples from the eight aquifer wells at the SDA generally are a calcium magnesium bicarbonate type (Knobel et al., 1992, 1997), which is typical of most water in the Snake River Plain aquifer. Water samples from three wells at the SDA were slightly enriched with Na plus K, and water from two wells were slightly enriched with Cl^- (Knobel et al., 1997, p. 20).

Median saturation indices indicate undersaturation of the waters with respect to fluorite, celestite, and gypsum. Primary silicates such as diopside, clinoenstatite, and olivine would also be expected to dissolve, where present. Dissolved silica concentrations range from 26 to 34 mg L^{-1}, and the water is slightly undersaturated with respect to silica glass to slightly supersaturated with respect to cryptocrystalline chalcedony (Knobel et al., 1992, 1997, p. 20–24).

Most groundwaters at the INEEL site have dissolved O_2, which restricts the extent to which redox conditions can vary at least in mobile uncontaminated waters at the site. Natural organic matter can be present in some of the less hydraulically conductive materials at the site, thereby potentially resulting in reducing conditions in some isolated, relatively immobile waters at the site. Combined with the fact that contaminated source areas can be expected to be associated with reducing waters, this implies a high degree of spatial heterogeneity of redox and other chemical conditions.

Investigations of cores collected at the site indicate that (i) calcite occurs both in fractures and in the sedimentary interbeds; (ii) iron oxyhydroxides, which can adsorb actinides strongly in certain conditions, are commonly observed on fracture surfaces and in the interbed sediments; and (iii) clay minerals, most commonly identified as illite, account for an average of 20% of the interbed sediments analyzed (Bartholomay, 1990b). Both smectite and mixed-layer smectite clays were observed in some interbed samples; these have the largest cation exchange capacities (CEC) of the clay minerals present. Samples from the SDA with low CECs contained clay minerals of illite, while high CEC samples contained from 9 to 33% expandable layer clays, mixed layer clays, and smectite (Rightmire and Lewis, 1987b).

These characteristics define an environment that controls the geochemical processes that affect contaminant mobility. For example, the presence of O_2 and C affects the oxidation–reduction characteristics of the system and hence the affinity of the chemical species for the aqueous or solid phase. Oxygen in the vadose zone at the SDA may be depleted by reaction with organic materials buried in the pits and trenches, creating localized reducing conditions and environments where some forms of Pu are more mobile than others. The mineralogy, size, consolidation, and fracture pattern of the solid-phase matrix and the chemical composition of the aqueous solution will affect the rate and amount of sorption and subsequent solute transport.

Transport of Contaminants as Solutes

Solute transport of radionuclides in the saturated and unsaturated zones at the INEEL depends strongly on reactive processes. The chemistry of infiltrating waters and of the contaminant source environment determines the extent of solubilization of the radionuclides. The aqueous speciation of the radionuclides and the evolution of this speciation as contaminated water encounters different mineral, surface, and fluid phases also affect radionuclide mobility. Retardation of radionuclides occurs because of their partitioning between the mobile phases (dissolved phase or mobile colloidal phase) and immobile phases. The immobile phases can be solid phases that incorporate contaminants and are precipitated from the aqueous solution, or can be mineral surfaces that sorb contaminants. In the latter case, it is important to distinguish two different types of sorption reactions: (i) ion exchange reactions, which occur on fixed-charge surfaces (such as smectite-clay interlayers) and mostly affect simple cationic species (such as Ca^{2+}, Na^+, Sr^{2+}, Cs^+, and possibly Am^{3+}), and (ii) surface complexation reactions, which occur on variable-charge surfaces (such as iron oxides, aluminum oxides, and silica) and can sorb a variety of aqueous species (cations, anions, neutral species, complexes), such as NpO_2^-, PuO_2OH^0, and UO_2^{+2}. In the case of sorption on variable charge surfaces, the speciation of the aqueous solution and its pH and redox conditions affect not only the distribution of aqueous species, but also the charge of the contacting surface and its ability to sorb given aqueous species. Thus redox conditions and variables such as the pH of the water and the concentration of both organic and inorganic complexing solutes strongly affect the aqueous stability and mobility of contaminants, and generally must be evaluated in predictions of reactive transport.

The partitioning reactions are thermodynamically driven. Their direction and extent are affected by the aqueous activity (also sometimes referred to as the "effective" concentration) of individual aqueous species, and at best only indirectly by the total aqueous concentration of all species of a contaminant. The activity of an aqueous species is dependent on the activities of all the other aqueous species in solution, both as a result of direct interactions between the various species (and consequent formation of ion pairs and complexes) and as a result of their overall effect on water molecule structures.

Chemical elements often have several oxidation states which may exhibit markedly different aqueous stabilities. For example, Pu occurs in four different oxidation states: III, IV, V, and VI. Pu(IV) is the oxidation state usually with the smallest aqueous stability (i.e., lowest affinity for the water phase) and is normally not very mobile as a solute. Pu(III), Pu(V), and Pu(VI) have significantly greater aqueous stabilities than Pu(IV), in large part because of their propensity to form strong aqueous complexes with carbonate ions. This significantly increases their mobility. Significant amounts of different oxidation states of a given element may coexist in an aqueous solution. The distribution of the oxidation states and the species of a contaminant generally depend on overall redox conditions, and are affected by the concentrations of major redox-active species such as dissolved O_2, sulfate/sulfide species, Fe(II)/Fe(III) species, Mn(II) species, dissolved organic C, and dissolved methane. Redox reactions, however, often have kinetic limitations that prevent redox equilibrium from being achieved (among various redox-active species), particularly if there is no microbial catalysis. Describing the potential changes in the redox speciation and transport of contaminants often requires knowledge of the identity and quantity of specific chemical species, products, and reactants, in addition to their reaction kinetics in relation to transport velocities. This is an area where there are many uncertainties and gaps in understanding related to contaminant reactions and transport. Generally, though, actinides are less mobile under reducing conditions (i.e., in their reduced oxidation states) than in the presence of oxidizing, oxygenated conditions.

Predicting the transport and potential immobilization of redox-active radionuclides in such an environment is difficult because of this spatial heterogeneity and because of uncertainties regarding the chelating properties of the mixed organic–radionuclide waste. It is generally thought that organic complexes may dominate the speciation of trivalent actinides, such as Am(III), whereas inorganic complexes such as carbonate and hydroxide species dominate the speciation of pentavalent and hexavalent actinides, such as Pu, Np, and U.

Speciation calculations (Curtis et al., 2003) using uncontaminated oxygenated groundwaters from the INEEL site with added trace amounts of either Pu, Np, U, or Am generally show that either Pu(V), mostly in the form of the $PuO_2CO_3^-$ aqueous species, or Pu(VI), mostly in the form of the $PuO_2CO_3^0$ aqueous species, should be the dominant oxidation state (depending on which of two thermodynamic databases is used for the calculations). Similarly, U(VI) is expected to be dominant, mostly in the form of either $UO_2(CO_3)_3^{-4}$ or $UO_2(CO_3)_2^{-2}$ aqueous species. According to the calculations, Np(V) should be the dominant oxidation state of Np, primarily in the form of the NpO_2^+ and $NpO_2CO_3^-$ species. The only exception is the speciation of perched water from an SDA well with the HATCHES database, which predicts a dominance of Np(VI) primarily in the form of the $NpO_2(CO_3)_3^{-4}$ complex. Similar speciation calculations, which didn't account for possible complexing by organic ligands, also indicate the importance of carbonate as a complexant for Am, particularly in the form of $AmCO_3^+$. The speciation calculations, however, are only generally indicative of the possible speciation of these radionuclides in the otherwise uncontaminated waters at the site.

Partitioning calculations modeling surface complexation reactions on variable charge surfaces (primarily goethite, but also ferrihydrite, quartz, montmorillonite, and alumina) were performed using Pu, Np, U, and Am as example contaminant radionuclides (Curtis et al., 2003; Landa et al., 2003). The simulations showed that even given a restricted set of conditions, such as the fairly similar water chemistries that were used to represent uncontaminated INEEL site waters, the partitioning of the radionuclides varied widely, for U by as much as 3000% The calculations also demonstrated the importance, and sensitivity, of the calculations to observed or postulated redox conditions, to pH and equilibrium pCO_2 levels (and consequently to dissolved carbonate concentrations), and finally showed that even under a uniform set of conditions, the extent of partitioning increases nonlinearly with increasing radionuclide concentrations, with generally stronger sorption affinities at lower concentrations.

Results presented by Landa et al. (2003) clearly indicate that although the evolution of an observed radionuclide plume may sometimes be backfitted using an empirical sorption model (such as the constant K_d or even the nonlinear Langmuir or Freundlich models), such models cannot generally be considered suitable for predicting contaminant transport. This pertains especially to the general case of dynamically evolving contaminant plumes and systems, where the composition and sorption potential of minerals and of their surfaces varies both spatially and temporally at any given point. This is not surprising given the complex web of dependences in multispecies reaction systems discussed above. The issue of the validity of empirical sorption models was addressed by Reardon (1981) and was reevaluated more recently by Glynn (2003), who used a surface complexation model to simulate competitive sorption reactions in one-dimensional transport simulations. This latter study, which used transport of Np and Pu as an example, also documented the effect of spatially heterogeneous sorption capacity distributions. The results, both for spatially uniform and for heterogeneous columns, differed markedly from results that would have been obtained in transport simulations using empirical sorption models (constant K_d, Langmuir, or Freundlich). When possible, the simulation breakthrough curves obtained were fitted to a constant K_d advection–dispersion transport model and compared. Functional differences often were great enough to prevent a meaningful fit of all the simulation results with a constant K_d (or even a Langmuir or Freundlich) model, even in the case of Np, which showed only weak sorption (and weak retardation) under the simulation conditions. Functional behaviors that could not be fitted included concentration trend reversals and radionuclide desorption spikes. In some cases, the simulation results were fitted successfully, but the fitted parameters (the apparent K_d and dispersivity values) varied significantly depending on simulation conditions. Perhaps most notably, Glynn (2003) demonstrated that a linear increase in the standard deviation of a specified sorption capacity distribution (modeled as a lognormal distribution) resulted in an exponential increase in the dispersion of the radionuclides.

Transport of Contaminants as Colloids

Transport of contaminants in the subsurface beneath the SDA could be enhanced by association with colloids and larger particles capable of being transported by water. In this paper we define a colloid as any nonaqueous-phase material capable of being mobile in the porous subsurface. Colloids can be rock and mineral fragments, mineral precipitates such as iron oxides and carbonates, weathering products such as clay minerals, macromolecular components of DOC such as humic substances, biocolloids such as microorganisms, and microemulsions of nonaqueous-phase liquids.

Colloids are present in the basalt fractures at INEEL and also have been measured in groundwater. The tighter packed interbed sediments beneath the SDA could inhibit transport of colloids by filtration; however, colloid transport through the coarser fractures is a possibility. Detections of Pu and Am in the interbeds at INEEL may indicate colloid-facilitated transport or transport as water soluble complexes.

The mobility of inorganic colloids in the subsurface is controlled by chemical interactions between colloids and immobile matrix surfaces, and hydrological and physical factors. Changes in aqueous chemistry can cause colloids to aggregate, thereby creating larger, less mobile particles. Changes in aqueous chemistry can also destabilize such aggregates resulting in smaller, more mobile colloids. For example, higher ionic strengths usually favor colloid aggregation; a decrease in ionic strength can destabilize colloids (McDowell-Boyer et al., 1986). Destabilization of colloids is also facilitated by pH-induced changes in surface charge or by the presence of strongly binding ions that decrease the net surface charge (McCarthy and Degueldre, 1993). Dissolution of a more soluble matrix surrounding the colloids can also lead to mobilization (Buddemeier and Hunt, 1988). Changes in redox conditions can lead to the formation or dissolution of colloids such as ferric hydroxide and can also affect the solubility of redox sensitive metal hydroxides, which may act as a cement for other colloids. Particles can be removed through mechanical filtration by smaller pore spaces, or released into groundwater as a result of mechanical grinding of mineral surfaces. Hydrodynamic forces associated with increases in groundwater velocity can dislodge colloids (Buddemeier and Hunt, 1988).

Aqueous-phase actinides can form colloids by hydrolysis and precipitation. These reactions are affected by actinide concentration, Eh, pH, and the concentration of complexing agents such as carbonate, phosphate, sulfate, and fluoride. For example, increasing the pH of Pu and Am solutions led to colloid formation at pH values between 7 and 9 (Ramsay, 1988). Americium solubility is at a minimum at pH 8, and addition of carbonate was found to cause precipitation of an $AmOHCO_3$ precipitate (Vilks and Drew, 1986).

Actinides have been shown to form colloid-sized complexes with organic molecules. Sheppard and Kittrick (1983) observed Am complexes with humic acid in the 1- to 10-nm size range. Nelson et al. (1985) determined that colloidal organic C and natural sediments used in laboratory experiments had approximately equal affinities for Pu(III+IV). Once complexed with colloidal organic C, the Pu was mobile and unavailable for sorption by the natural sediments. Sheppard et al. (1980a, 1980b) found evidence for U and Am complexes with humic molecules in the 1- to 60-nm size range.

The association of actinides with colloidal organic C can be a potentially effective method for mobilization and transport beneath the SDA. Reducing conditions caused by degradation of organic wastes can mobilize colloids as well as solutes. Vilks et al. (1998) put compacted organic waste into airtight steel containers filled with water. After 18 mo, the aged leachate contained 5 to 110 mg L^{-1} organic colloids. The reducing environment can also cause mobilization of Fe(II). Upon mixing with oxygenated water, Fe(II) may form colloidal iron oxides, which have a large capacity for adsorption of some chemical species.

Americium, Np, Pu, and U oxides and hydroxides can exist as colloids in groundwater (McCarthy and Degueldre, 1993). There is also evidence for transport of actinides as colloids during column experiments (e.g., Seitz et al., 1978; Champ et al., 1982; Fjeld et al., 1998). In these experiments the highest concentrations of Am(III) and Pu(IV) were located near the inlet of the columns, indicating adsorption and/or precipitation. However, a small fraction of both elements eluted at almost the same rate as a nonreactive tracer, indicating transport as a colloid. Generally, the form of the actinide eluting from the columns was not determined, so whether the fast elution was facilitated by transport as a colloid or transport as an aqueous complex was undetermined. In some experiments, however, secondary evidence implicated transport as a colloid.

Column experiments were conducted by Newman et al. (1995) to evaluate transport of Am, Pu, and U in the subsurface at INEEL. Columns were packed with

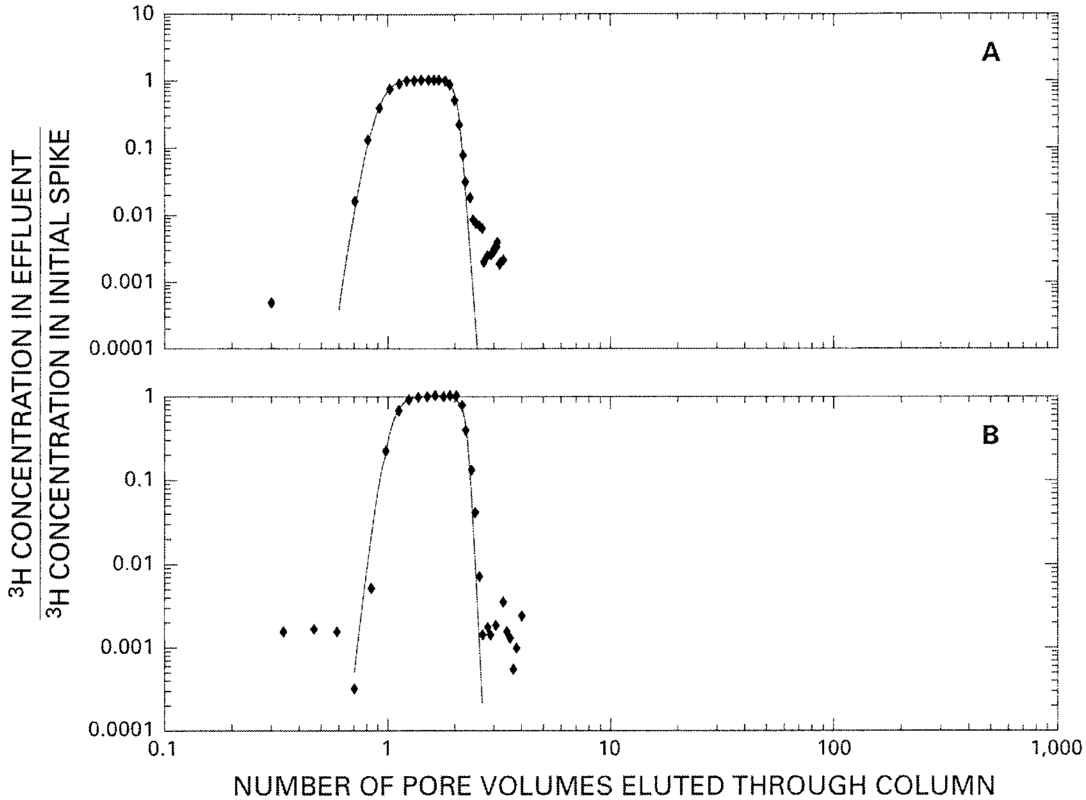

Fig. 9. Breakthrough of ^{3}H transported through packed columns of (a) crushed basalt and (b) sediments (Newman et al., 1995). Point symbols represent measured concentrations; the solid curve represents model simulations.

either a crushed basalt or a composite of sediment interbed samples. Synthetic groundwater was used as the eluent; the composition was based on analyses from the eastern Snake River Plain aquifer (Wood and Low, 1986). Approximately one pore volume of synthetic groundwater containing Pu was put through each column, followed by leaching with 200 pore volumes of Pu-free groundwater. Tritium was added to evaluate transport of a conservative tracer and determine if preferential channeling occurred in either column. A one-dimensional advective–dispersive transport model was used to simulate tritium and Pu transport through both columns. Figures 9a and 9b show breakthrough of tritium from the crushed basalt and sediment interbed columns. The one-dimensional model simulations of tritium breakthrough match the observed results, indicating conservative transport and the absence of channeling. Breakthrough of Pu from the crushed basalt column was characterized by an initial peak, approximately coinciding with that of tritium, followed by a gradual decrease in concentration (Fig. 10a). The model simulation indicated that this peak in Pu concentration was a result of conservative transport. There was also an initial increase in Pu in leachate from the interbed sediment column (Fig. 10b), although concentrations were significantly lower than in leachate from the crushed basalt column.

Independent batch experiments with both the crushed basalt and interbed sediments indicated significant sorption of Pu. The initial increases in Pu concentration from both columns at almost the same time as tritium breakthrough were much faster than predicted from the equilibrium-based distribution coefficients obtained from the batch experiments (Newman et al., 1995), suggesting colloidal transport. The data were insufficient, however, to determine whether Pu occurred as discrete colloidal precipitates, or was sorbed on a mobile colloidal phase. It should be noted that the colloidal particles formed during crushing of the basalt may not be representative of colloids in the vadose zone at INEEL. Even so, the crushed basalt column experiments do indicate the possibility of colloid-facilitated transport.

Colloid facilitated transport of actinides in the field also has been documented. Plutonium and Am were found beneath and downgradient from waste-disposal beds at Los Alamos, NM at distances that indicate colloid facilitated transport (Nyhan et al., 1985; Penrose et al., 1990; Nuttall et al., 1991). Arguments, although controversial, also suggest that there also is evidence for migration of Pu as a colloid at the Nevada Test Site (Kersting et al., 1999). Isotopic ratios show that Pu measured in groundwater had traveled 1.3 km from the site of a particular underground explosion. The 30-yr travel time is consistent with the travel time for groundwater in the area. Uranium associated with colloidal kaolinite and silica has been detected in groundwater from Australia (Payne et al., 1992).

There is abundant evidence for transport of colloid and larger size particles at INEEL. Interconnected fractures in basalt cores beneath SDA are reported to contain abundant sediment infill ranging in size from clay- to sand-sized particles; mineral precipitates including

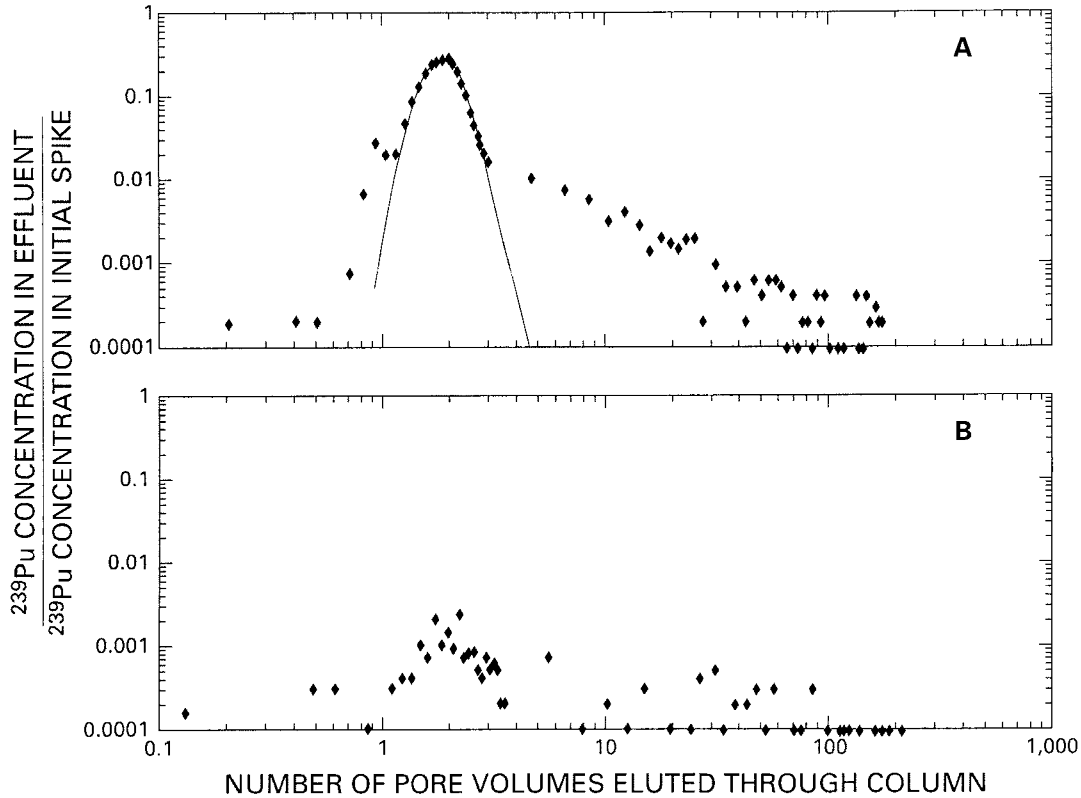

Fig. 10. Breakthrough of ^{239}Pu transported through packed columns of (a) crushed basalt and (b) sediments (Newman et al., 1995). Point symbols represent measured concentrations; the solid curve represents model simulations.

calcite, iron oxides, and amorphous silica are also present (Rightmire and Lewis, 1987a). These infill minerals likely result from a combination of in situ precipitation and filtering out of colloids from a flowing phase. Periodic transmission of relatively large quantities of water are capable of transporting colloids through the vadose zone. However, it is not clear what fraction of the sediment infill was deposited between lava flows as opposed to transport by modern-day infiltration. As stated earlier in this paper, seasonal streamflow, snowmelt, and local runoff periodically generate large quantities of infiltrating water which can potentially transport colloids and any associated contaminants deeper in the subsurface. Estes and McCurry (1994) measured colloid concentrations ranging from 1.8 to 9.8 mg L^{-1} in groundwater at INEEL. Electron microscopy–energy-dispersive X-ray microscopy analysis of filter membranes suggest the colloids consisted of carbonates, iron oxides, and clay minerals. Rees and Cleveland (1982) measured Pu concentrations in four wells around the INTEC. Plutonium concentrations were above their detection limit of 10 fCi L^{-1} in only one well. About 25% of the Pu was removed by 0.05-μm filtration, suggesting association with colloids. The remaining 75% was in true solution, or present as fine colloidal particles smaller than 0.05 μm.

A significant problem in studying colloid transport in the field is ensuring that the colloids recovered from a well are representative of conditions in the aquifer. Drilling redistributes material, creates fine particles, and introduces materials such as drilling mud. Sampling procedures can introduce artifacts, including the removal of existing colloids attached to the immobile solid phase, creation of colloids during sampling, creation of colloids during separation from solution, or changes in the chemical and physical properties of natural colloids as a result of alteration in O_2 and CO_2 content, temperature, pH, Eh, and light as groundwater is brought to the surface. Nucleation and precipitation of colloids on filter material can be mistakenly interpreted to indicate the presence of colloids in a water sample.

CONCLUDING REMARKS

The geologic framework at the INEEL is complex, comprising granular media and consolidated, fractured rock. These media are highly stratified. The framework is characterized by extreme heterogeneity and anisotropy. The contrasts in properties of adjacent layers may impede downward flow but also may lead to various types of fast or preferential flow. Contaminant mobility in these media is influenced by diverse constituents and conditions that vary in space and time, including redox conditions, concentrations of organic and inorganic complexing solutes, and the aqueous speciation of contaminants such as actinides.

Various locations within the INEEL, notably the SDA, have been the focus of intensive subsurface characterization since the 1950s. Most recently these studies have included predictive modeling to evaluate the behavior of contaminants in the subsurface and the risks associated with these contaminants.

Table 2. Important features and processes relevant to the issue of buried waste at the SDA.

Feature/process	Favorable aspects	Unfavorable aspects	Complicating factors
Thick vadose zone	Long travel times to aquifer under unsaturated conditions; much material for possible sorption	Large zone of poorly understood phenomena	Difficult to (i) conduct meaningful field experiments, (ii) differentiate among flow processes within layers, (iii) monitor dynamics of system in situ, (iv) recover sediment cores for analysis
Heterogeneity of basalt	High permeability increases dilution–dispersion; dense basalt slows flow	High permeability decreases travel times	Physical processes in basalts are poorly understood (e.g., unsaturated flow in fractures), sorption properties of sediment-filled fractures and vesicles have not yet been fully investigated
Continuous sedimentary interbeds	High density of sorption sites; low hydraulic conductivity	Enhanced horizontal spreading can take contaminants outside monitored area	Properties may not be adequately characterized (e.g., lack of measurements on coarse materials) to model these processes in a realistic way
Discontinuous sedimentary interbeds	Where interbeds are present: High density of sorption sites; low hydraulic conductivity	"Holes" provide fast pathways and permit bypassing of the sorptive interbeds	Continuity is not well known, especially where well density is low
Preferential flow	Promotes dispersal and dilution of contaminants	Decreases travel time; decreases the number of sorption sites to which contaminants are exposed	High degree of phenomenological complexity; processes are poorly understood and inadequately described by current models
Vertical heterogeneity	Slows vertical flow, especially under unsaturated conditions	Enhanced horizontal spreading can take contaminants outside monitored area	Particular well completion depths influence observations of perching; difficult to evaluate and implement adequate model resolution
Horizontal heterogeneity	Slows horizontal flow	Can preferentially direct flow to regions of high vertical conductivity	Information is difficult to obtain and little is available; effort required to incorporate into models
Anisotropy	Favors horizontal over vertical dispersal of contaminants within the vadose zone	Enhanced horizontal spreading can take contaminants outside monitored area	Enhances possibilities for horizontal movement, even if driving forces are small
Episodic large-magnitude infiltration	Contributes large input of water for dilution and dispersal	Decreases travel times	Difficult to predict; antecedent moisture conditions influence effects; generates preferential flow
Perching	Provides zone for enhanced mixing and dilution of contaminants	Enables fast horizontal transport	Extent and persistence are unknown in areas lacking monitoring wells
Solute transport	Dispersal promotes dilution and movement to any sorptive regions	Causes spread of contamination	Source term is highly uncertain; traditional models may not yield accurate results in a dynamic system
Preexisting chemistry (unaffected by introduction of contaminants)	Prevailing oxidizing conditions inhibit some types of solute transport	Contrasts with the anthropogenically altered conditions may increase some forms (e.g., colloidal) of contaminant transport	At some locations the preexisting chemistry may be difficult to assess
Spatial geochemical heterogeneity	Increased dispersion promotes dilution and movement to any sorptive regions	Increased dispersion increases spreading; decreased retardation	There are many sources of heterogeneity; heterogeneity exists at diverse scales
Temporal geochemical variability	Greater variety of processes increases the likelihood that contaminants will encounter sorptive processes	Can allow immobilized contaminants to remobilize	Temporal variability depends on hydraulic conditions and their variation in time and space
Colloid transport	Filtration processes limit colloid mobility	Allows convective transport of adsorbed chemical	Adsorptive characteristics of colloids are poorly understood; depends strongly on solution chemistry and redox conditions

Our summary of major features and processes relevant to the issue of contaminant transport at the INEEL is in Table 2. The table lists the most noteworthy favorable, unfavorable, and complicating factors of the specific features. The listed complicating factors mainly relate to difficulties in evaluating the feature's influence. From the perspective of minimizing hazards from environmental contamination, favorable circumstances would include (i) mobilization from contaminant sources at low concentrations over a long time; (ii) a chemical environment that facilitates dispersion, dilution, sorption, and precipitation; (iii) chemical and geologic environments that are not conducive to colloid formation; (iv) dispersion of contaminants within the vadose zone; (v) diffuse flow of water; (vi) long travel times within the vadose zone; (vii) abundant sorption sites; and (viii) immobilization of colloids by filtration or other means. There is not only overlap but also some contradiction among these factors. One example is that conditions that inhibit solute transport may be favorable for colloid transport.

Another is that while vadose zone dispersion increases the number of sorption sites to which contaminants are exposed, it tends to transport contaminants beyond localized regions where they might be more easily monitored or treated. Given the scope and complexity of the problem of reducing environmental contamination risks, contradictory considerations like these are inherent. Thus it is unavoidable that they appear in this summary.

Innumerable research topics are viable for expanding available knowledge of the hydraulic and geochemical framework at the INEEL. Areas we perceive to be particularly valuable for understanding the dynamic subsurface transport system and evaluating its effect on contamination-related risks include the following:

- Colloids—in what concentrations are they present? To what extent do they incorporate contaminants? How far do they move? Do they get remobilized during subsequent recharge events, or trapped in small pore spaces?
- Dynamics of flow (i.e., infiltration, ET, residence times, preferential flow) in the surficial sediments and sedimentary interbeds—how does this affect contaminant mobilization and transport? What phenomena are important and how can they be quantified?
- Actinides in the surficial sediments—are they mobilized upon reduction of organic wastes in which they are contained? What is their aqueous speciation? Will they remain in solution or sorb onto immobile materials? Will they form precipitates that may be transported as colloids? Will actinides sorb onto other potentially mobile colloids such as iron oxides, clay minerals, and carbonates?
- Physical diffusion to sorption sites—to what extent is this a limiting factor for sorption or other retarding processes?
- Basalt flows and their contacts with the interbeds—how do their structural elements relate to subsurface transport? What is the nature of flow within the fractured medium? What is the nature of rubble zones and how widespread are they?
- Nonequilibrium chemistry—what is the best way to treat this in predictive studies?
- Substantial horizontal vadose zone flow—what is its net effect on contaminant transport?

Investigations on these topics can productively build on the scientific knowledge already developed to increase understanding of vadose zone systems in general as well as to address hazard-related needs at the INEEL site.

REFERENCES

Ackerman, D.J. 1995. Analysis of steady-state flow and advective transport in the Eastern Snake Plain aquifer system. U.S. Geological Survey Water Resources Investigations Rep. 94-4257:25. USGS, Idaho Falls, ID.

Anderson, S.R. 1991. Stratigraphy of the unsaturated zone and uppermost part of the Snake River Plain aquifer at the Idaho Chemical Processing Plant and Test Reactors Area, Idaho National Engineering Laboratory, Idaho. USGS Water-Resources Investigations Rep. 91-4010 (DOE/ID-22095). USGS, Idaho Falls, ID.

Anderson, S.R., D.J. Ackerman, M.J. Liszewski, and R.M. Freiburger. 1996. Stratigraphic data for wells at and near the Idaho National Engineering Laboratory, Idaho. USGS Open-File Rep. 96-248 (DOE/ID-22127). USGS, Idaho Falls, ID.

Anderson, S.R., M.A. Kuntz, and L.C. Davis. 1999. Geologic controls of hydraulic conductivity in the Snake River Plain aquifer at and near the Idaho National Engineering and Environmental Laboratory, Idaho. USGS Water Resources Investigations Rep. 99-4033 (DOE/ID-22155). USGS, Idaho Falls, ID.

Anderson, S.R., and B.D. Lewis. 1989. Stratigraphy of the unsaturated zone at the radioactive waste management complex, Idaho National Engineering Laboratory, Idaho. USGS Water Resources Investigations Rep. 89–4065 (DOE/ID-22080). USGS, Idaho Falls, ID.

Anderson, S.R., and M.J. Liszewski. 1997. Stratigraphy of the unsaturated zone and the Snake River Plain aquifer at and near the Idaho National Engineering Laboratory, Idaho. USGS Water Resources Investigations Rep. 97-4183 (DOE/ID-22142). USGS, Idaho Falls, ID.

Barraclough, J.T., J.B. Robertson, and V.J. Janzer. 1976. Hydrology of the solid waste burial ground as related to the potential migration of radionuclides, Idaho National Engineering Laboratory. USGS Open-File Rep. 76-471. USGS, Idaho Falls, ID.

Barraclough, J.T., W.E. Teasdale, and R.G. Jensen. 1967. Hydrology of the National Reactor Testing Station, Idaho, 1965. USGS Open-File Rep. IDO-22048. USGS, Idaho Falls, ID.

Bartholomay, R.C. 1990a. Mineralogy, petrology, and grain size of surficial sediment from the Big Lost River, Little Lost River and Birch Creek drainages, Idaho National Engineering Laboratory, Idaho. M.S. thesis. Idaho State University, Pocatello.

Bartholomay, R.C. 1990b. Mineralogical correlation of surficial sediment from area drainages with selected sedimentary interbeds at the Idaho National Engineering Laboratory, Idaho. USGS Water Resources Investigations Rep. 90-4147 (DOE/ID-22092). USGS, Idaho Falls, ID.

Bartholomay, R.C. 1990c. Digitized geophysical logs for selected wells on or near the Idaho National Engineering Laboratory, Idaho. USGS Open-File Rep. 90-366 (DOE/ID-22088). USGS, Idaho Falls, ID.

Bartholomay, R.C. 1998. Distribution of selected radiochemical and chemical constituents in perched ground water, Idaho National Engineering Laboratory, Idaho, 1992–95. USGS Water Resources Investigations Rep. 98-4026 (DOE/ID-22145). USGS, Idaho Falls, ID.

Bartholomay, R.C., L.L. Knobel, and L.C. Davis. 1989. Mineralogy and grain size of surficial sediment from the Big Lost River drainage and vicinity, with chemical and physical characteristics of geologic materials from selected sites at the Idaho National Engineering Laboratory, Idaho. USGS Open File Rep. 89-384. USGS, Idaho Falls, ID.

Bartholomay, R.C., and B.J. Tucker. 2000. Distribution of selected radiochemical and chemical constituents in perched ground water, Idaho National Engineering and Environmental Laboratory, Idaho, 1996–98. U.S. Geological Survey Water Resources Investigations Rep. 00-4222. (DOE/ID-22168). USGS, Idaho Falls, ID.

Beasley, T.M., P.R. Dixon, and L.J. Mann. 1998b. Tc-99, U-236, and Np-237 in the Snake River Plain Aquifer at the Idaho National Engineering and Environmental Laboratory, Idaho Falls, Idaho, U.S.A. Environ. Sci. Technol. 32:3875–3881.

Beasley, T.M., J.M. Kelley, L.A. Bond, W. Rivera, Jr., M.J. Liszewski, and K.A. Orlandini. 1998a. Heavy element radionuclides (Pu, Np, U) and ^{137}Cs in soils collected from the Idaho National Engineering and Environmental Laboratory and other sites in Idaho, Montana, and Wyoming. U.S. Department of Energy EML-599. USDOE, Washington, DC.

Bechtel BWXT Idaho. 2002. Vadose zone instrumented well and borehole installations near the new INTEC percolation pond area end of well reports: Idaho National Engineering and Environmental Laboratory. Environmental Restoration Directorate Rep. INEEL/EXT-02-00085. INEEL, Idaho Falls, ID.

Becker, B.H., J.D. Burgess, K.J. Holdren, D.K. Jorgensen, S.O. Magnuson, and A.J. Sondrup. 1998. Interim risk assessment and contaminant screening for the Waste Area Group 7 remedial investigation. DOE/ID-10569, Draft rev. 2. Lockheed Martin Idaho Technologies Company, Idaho Falls, ID.

Bishop, C.W. 1991. Hydraulic properties of vesicular basalt. M.S. thesis. University of Arizona, Tucson.

Bishop, C.W. 1996. Soil moisture monitoring results at the Radioactive Waste Management Complex of the Idaho National Engineering Laboratory, FY-96, FY-95, and FY-94. INEL-96/297. Lockheed Martin Idaho Technologies Company, Idaho Falls, ID.

Borghese, J.V. 1991. Hydraulic characteristics of soil cover, Subsurface Disposal Area, Idaho National Engineering Laboratory. M.S. thesis. University of Idaho, Pocatello.

Brooks, R.H., and A.T. Corey. 1964. Hydraulic properties of porous media. Colorado State University Hydrology Paper 3. Colorado State University, Fort Collins.

Buddemeier, R.W., and J.R. Hunt. 1988. Transport of colloidal contaminants in groundwater: Radionuclide migration at the Nevada Test Site. Appl. Geochem. 3:535–548.

Burgess, J.D., B.D. Higgs, and T.R. Wood. 1994. WAG 7 groundwater pathway track 2 summary report. EGG-ER-10731. EG&G Idaho, Idaho Falls, ID.

Busenberg, E., L.N. Plummer, and R.C. Bartholomay. 2001. Estimated age and source of the young fraction of ground water at the Idaho National Engineering and Environmental Laboratory. USGS Water Resources Investigations Rep. 01-4265. USGS, Idaho Falls, ID.

Busenberg, E., L.N. Plummer, M.W. Doughten, P.K. Widman, and R.C. Bartholomay. 2000. Chemical and isotopic composition and gas concentrations of ground water and surface water from selected sites at and near the Idaho National Engineering and Environmental Laboratory, Idaho, 1994–97. USGS Open-File Rep. 00-81. USGS, Idaho Falls, ID.

Busenberg, E., E.P. Weeks, L.N. Plummer, and R.C. Bartholomay. 1993. Age dating ground water by use of chlorofluorocarbons (CCl3F and CCl2F2), and distribution of chlorofluorocarbons in the unsaturated zone, Snake River Plain aquifer, Idaho National Engineering Laboratory, Idaho. USGS Water Resources Investigations Rep. 93-4054 (DOE/ID-22107). USGS, Idaho Falls, ID.

Cecil, L.D., B.R. Orr, T. Norton, and S.R. Anderson. 1991. Formation of perched ground-water zones and concentrations of selected chemical constituents in water, Idaho National Engineering Laboratory, Idaho 1986–88. USGS Water Resources Investigations Rep. 91–4166 (DOE/ID-22100). USGS, Idaho Falls, ID.

Cecil, L.D., J.R. Pittman, T.M. Beasley, R.L. Michel, P.W. Kubik, P. Sharma, U. Fehn, and H.E. Gove. 1992. Water infiltration rates in the unsaturated zone at the Idaho National Engineering Laboratory estimated from chlorine-36 and tritium profiles, and neutron logging, p. 709–714. *In* Y. Kharaka and A. Maest (ed.) Water rock interaction. Balkema, Rotterdam, the Netherlands.

Champ, D.R., W.F. Merritt, and J.L. Young. 1982. Potential for the rapid transport of plutonium in groundwater as demonstrated by core column studies. p. 745–754. *In* Scientific basis for nuclear waste management. Materials Research Society, Pittsburgh, PA.

Clawson, K.L., G.E. Start, and N.R. Ricks. 1989. Climatography of the Idaho National Engineering Laboratory. 2nd ed. DOE/ID-12118. U.S. Department of Energy Idaho Operations, Idaho Falls, ID.

Colello, J.J., J.J. Rosentreter, R.C. Bartholomay, and M.J. Liszewski. 1998. Strontium distribution coefficients of basalt core samples from the Idaho National Engineering and Environmental Laboratory, Idaho. U.S. Geological Survey Water Resources Investigations Rep. 98-4256 (DOE/ID-22153). USGS, Idaho Falls, ID.

Curtis, G.P., P.D. Glynn, K.G. Stollenwerk, and R.C. Bartholomay. 2003. Actinide transport processes. *In* J.P. Rousseau et al. (ed.) Review of the transport of selected radionuclides in the Interim Risk Assessment for the Radioactive Waste Management Complex, Waste Area Group 7, Operable Unit 7-13/14, Idaho National Engineering and Environmental Laboratory, Idaho. Administrative Report. USGS, Idaho Falls, ID.

Davis, L.C., S.R. Hannula, and B. Bowers. 1997. Procedures for use of, and drill cores and cuttings available for study at, the Lithologic Core Storage Library, Idaho National Engineering Laboratory, Idaho. USGS Open-File Rep. 97-124 (DOE/ID-22135). USGS, Idaho Falls, ID.

Davis, L.C., and J.R. Pittman. 1990. Hydrological, meteorological, and geohydrological data for an unsaturated zone study near the Radioactive Waste Management Complex, Idaho National Engineering Laboratory, Idaho—1987. USGS Open-File Rep. 90-114. USGS, Idaho Falls, ID.

Dunnivant, F.M., M.E. Newman, C.W. Bishop, D. Burgess, J.R. Giles, B.D. Higgs, J.M. Hubbell, E. Neher, G.T. Norrell, M.C. Pfiefer, I. Porro, R.C. Starr, and A.H. Wyllie. 1998. Water and radioactive tracer flow in a heterogeneous field-scale system. Ground Water 36:949–958.

Estes, M., and M. McCurry. 1994. Concentrations and compositions of colloidal particles in ground water near the ICPP, Idaho National Engineering Laboratory, Idaho. p. 165–179. *In* Proceedings, 30th Symposium Engineer's Geology of Geotechnical Engineering–Hydrogeology Waste Disposal—Science and Politics, Pocatello, ID. Society for Mining Metallurgy and Exploration, Littleton, CO.

Fjeld, R.A., J.T. Coates, A.W. Elzerman, and J.K. Navratil. 1998. Column studies of plutonium transport in sedimentary interbeds from the Snake River Plain, p. 7. *In* Proceedings of Waste Management 98 Symposium, Tucson, AZ. 1–5 Mar. 1998.

Forman, S.L., R.P. Smith, W.R. Hackett, J.A. Tullis, and P.A. McDaniel. 1993. Timing of late Quaternary glaciations in the western United States based on the age of loess on the eastern Snake River Plain, Idaho. Quat. Res. 40:30–37.

French, D.L., and K.A. Taylor. 1998. Radioactive waste information for 1997 and record-to-date. DOE/ID-10054(97). Waste Generator Services, Lockheed Martin Idaho Technologies, Idaho Falls, ID.

Garabedian, S.P. 1992. Hydrology and digital simulation of the regional aquifer system, eastern Snake River Plain, Idaho. USGS Prof. Pap. 1408-F. USGS, Denver, CO.

Geist, D.J., R.A. Ellisor, E.N. Sims, and S.S. Hughes. 2002. Subsurface volcanology at Test Area North and controls on groundwater flow. p. 45–59. *In* P.K. Link and L.L. Mink (ed.) Geology, hydrogeology, and environmental remediation—Idaho National Engineering and Environmental Laboratory, Eastern Snake River Plain, Idaho. Special Paper 353. Geological Society of America, Boulder, CO.

Geslin, J.K., P.K. Link, J.W. Riesterer, M.A. Kuntz, and C.M. Fanning. 2002. Pliocene and Quaternary stratigraphic architecture and drainage systems of the Big Lost Trough, northeastern Snake River Plain, Idaho. p. 11–26. *In* P. K. Link and L. L. Mink (ed.) Geology, hydrogeology, and environmental remediation—Idaho National Engineering and Environmental Laboratory, Eastern Snake River Plain, Idaho. Special Paper 353. Geological Society of America, Boulder, CO.

Gianniny, G.L., J.K. Geslin, J. Riesterer, P.K. Link, and G.D. Thackray. 1997. Quaternary surficial sediments on the Test Area North (TAN) area, northeastern Snake River Plain: An actualistic guide to aquifer characterization. p. 29–44. *In* S. Sharma and J.H. Hardcastle (ed.) Proc. of the 32nd Symp. on Engineering Geology and Soil Engineering, Boise, ID.

Glass, R.J., T.S. Steenhuis, and J.-Y. Parlange. 1989. Mechanism for finger persistence in homogeneous unsaturated, porous media: Theory and verification. Soil Sci. 148:60–70.

Glynn, P. 2003. Modeling Np and Pu transport with a surface complexation model and spatially variant sorption capacities: Implications for reactive transport modeling and performance assessments of nuclear waste disposal sites. Comput. Geosci. 3:331–349

Hendrickx, J.M.H., and T.-M. Yao. 1996. Prediction of wetting front stability in dry field soils using soil and precipitation data. Geoderma 70:265–280.

Holdren, K.J., B.H. Becker, N.L. Hampton, L.D. Koeppen, S.O. Magnuson, T.J. Meyer, G.L. Olson, and A.J. Sondrup. 2002. Waste Area Group 7 Operable Unit 7-13/14 Pre-Draft Remedial Investigation and Baseline Risk Assessment (DRAFT). DOE/ID-10995 Revision C. U.S. Department of Energy Idaho Operations Office, Idaho Falls, ID.

Hubbell, J.M. 1990. Perched ground water at the Radioactive Waste Management Complex of the Idaho National Engineering Laboratory. Rep. EGG-ER-8779. EG&G Idaho Inc., Idaho Falls, ID.

Hughes, J.D. 1993. Analysis of characteristics of sedimentary interbeds at the radioactive waste management complex at the Idaho National Engineering Laboratory. M.S. thesis. Idaho State University, Pocatello.

Hughes, S.S., R.P. Smith, W.R. Hackett, and S.R. Anderson. 1999. Mafic volcanism and environmental geology of the Eastern Snake River Plain, Idaho, p. 143–168. *In* S.S. Hughes and G. D. Thackray (ed.) Guidebook to the geology of Eastern Idaho. Idaho Museum of Natural History, Pocatello.

Humphrey, T.G., T.H. Smith, and M.C. Pope. 1982. Projected subsurface migration of radionuclides from buried Idaho National Engineering Laboratory transuranic waste. Nucl. Technol. 58:136–149.

Jury, W.A., W.R. Gardner, and W.H. Gardner. 1991. Soil Physics. 5th ed. Wiley, New York.

Kersting, A.B., D.W. Efure, D.L. Finnegan, D.J. Rokop, K.K. Smith, and J.L. Thompson. 1999. Migration of plutonium in groundwater at the Nevada Test Site. Nature 397:56–59.

Knobel, L.L., B.R. Orr, and L.D. Cecil. 1992. Summary of background concentrations of selected radiochemical and chemical constituents in groundwater from the Snake River Plain aquifer, Idaho–estimated from an analysis of previously published data. J. Idaho Acad. Sci. 28:48–61.

Knobel, L.L., L.D. Cecil, and T.R. Wood. 1995. Chemical composition of selected core samples, Idaho National Engineering Laboratory, Idaho. USGS Open-File Rep. 95-748 (DOE/ID-22126). USGS, Idaho Falls, ID.

Knobel, L.L., R.C. Bartholomay, and B.R. Orr. 1997. Preliminary delineation of natural geochemical reactions, Snake River Plain aquifer system, Idaho National Engineering Laboratory and vicinity, Idaho. USGS Water Resources Investigations Rep. 97-4093 (DOE/ID-22139). USGS, Idaho Falls, ID.

Knobel, L.L., L.D. Cecil, S. Fisher, and J.R. Green. 2001. Chemical composition of selected solid-phase samples from the Snake River Plain aquifer system and contributing drainages, eastern Idaho and western Wyoming. USGS Open-file Rep. 01-36. USGS, Idaho Falls, ID.

Knobel, L.L., R.C. Bartholomay, L.D. Cecil, B.J. Tucker, and S.J. Wegner. 1992. Chemical constituents in the dissolved and suspended fractions of ground water from selected sites, Idaho National Engineering Laboratory and vicinity, Idaho, 1989. USGS Open-File Rep. 92-51 (DOE/ID-22101). USGS, Idaho Falls, ID.

Knutson, C.F., K.A. McCormick, J.C. Crocker, M.A. Glenn, and M.L. Fishel. 1992. 3D RWMC vadose zone modeling (including FY-89 to FY-90 basalt characterization results). EGG-ERD-10246. EG&G Idaho, Inc., Idaho Falls, ID.

Kuntz, M.A., H.R. Covington, and L.J. Schorr. 1992. An overview of basaltic volcanism of the eastern Snake River Plain Idaho. p. 227–267. Geological Society of America Memoir 179. GSA, Boulder, CO.

Kuntz, M.A., and G.B. Dalrymple. 1979. Geology, geochronology, and potential volcanic hazards in the Lava Ridge-Hells Half Acre area, eastern Snake River Plain, Idaho. USGS Open-File Rep. 79-1657. USGS, Idaho Falls, ID.

Kuntz, M.A., G.B. Dalrymple, D.E. Champion, and D.J. Doherty. 1980. Petrography, age, and paleomagnetism of volcanic rocks at the Radioactive Waste Management Complex, Idaho National Engineering Laboratory, Idaho, with an evaluation of potential volcanic hazards. USGS Open-File Rep. 80-388. 63 p.

Kuntz, M.A., B. Skipp, M.A. Lanphere, W.E. Scott, K.L. Pierce, G.B. Dalrymple, D.E. Champion, G.F. Embree, W.R. Page, L.A. Morgan, R.P. Smith, W.R. Hackett, and D.W. Rodgers. 1994. Geologic map of the Idaho National Engineering Laboratory and adjoining areas, eastern Idaho: USGS Miscellaneous Investigations Map I-2330, scale 1:100 000. USGS, Idaho Falls, ID.

Kwicklis, E.M., and R.W. Healy. 1993. Numerical investigations of steady liquid water flow in a variably saturated fracture network. Water Resour. Res. 29:4091–4102.

Landa, E.R., P.D. Glynn, K.G. Stollenwerk, and G.P. Curtis. 2003. Distribution coefficients (K_ds) and their application to transport analysis. *In* J.P. Rousseau et al. (ed.) Review of the transport of selected radionuclides in the Interim Risk Assessment for the Radioactive Waste Management Complex, Waste Area Group 7, Operable Unit 7-13/14, Idaho National Engineering and Environmental Laboratory, Idaho. Administrative Report. USGS, Idaho Falls, ID.

Laney, P.T., S.C. Minkin, R.G. Baca, D.L. McElroy, J.M. Hubbell, L.C. Hull, B.F. Russell, G.J. Stormberg, and J.R. Pittman. 1988. Subsurface investigation program at the Radioactive Waste Management Complex of the Idaho National Engineering Laboratory. USDOE Idaho Operations Office Rep. DOE/ID-10183. USDOE, Idaho Falls, ID.

Leecaster, M.K. 2002. Geostatistic modeling of subsurface characteristics in the Radioactive Waste Management Complex Region, Operable Unit 7-13/14. INEEL/EXT- 02-00029.

Leenheer, J.A., and J.C. Bagby. 1982. Organic solutes in ground water at the Idaho National Engineering Laboratory. USGS Water Resources Investigation 82-15 (IDO-22061). USGS, Idaho Falls, ID.

Magnuson, S.O. 1995. Inverse modeling for field scale hydrologic and transport parameters of fractured basalt. INEL-95/0637. Lockheed Martin Idaho Technologies Company, Idaho Falls, ID.

Magnuson, S.O., and A.J. Sondrup. 1998. Development, calibration, and predictive results of a simulator for subsurface pathway fate and transport of aqueous- and gaseous-phase contaminants in the subsurface disposal area at the Idaho National Engineering Laboratory. INEEL/EXT-97-00609. Idaho National Engineering and Environmental Laboratory, Idaho Falls, ID, and Lockheed Martin Idaho Technologies Company, Idaho Falls, ID.

Markham, O.D. 1978. Activation and fission products in the environment near the Idaho National Engineering Laboratory Radioactive Waste Management Complex. USDOE IDO-12095. USDOE, Washington, DC.

McCarthy, J.M., and C. Degueldre. 1993. Sampling and characterization of colloids and particles in groundwater for studying their role in contaminant transport. p. 247–315. *In* J. Buffle and H.P. van Leeuwen (ed.) Environmental particles. Vol. 2. Lewis Publ., Boca Raton, FL.

McCarthy, J.M., and D.L. McElroy. 1995. SDA hydraulic characterization data compilation-surficial sediments and interbeds. Engineering Design File ER-WAG7-71, INEL-95/130. Lockheed Martin Idaho Technologies Company, Idaho Falls, ID.

McDowell-Boyer, L.M., J.R. Hunt, and N. Sitar. 1986. Particle transport through porous media. Water Resour. Res. 22:1901–1921.

McElroy, D., and J. Hubbell. 1990. Hydrologic and physical properties of sediments at the radioactive waste management complex. EGG-BG-9147. EG&G Idaho, Inc., Idaho Falls, ID.

McElroy, D.L., and J.M. Hubbell. 2003. Advanced tensiometer monitoring results from the deep vadose zone at the Radioactive Waste Management Complex. INEEL/EXT-02–01276. Idaho National Engineering and Environmental Laboratory, Bechtel BWXT Idaho, LLC, Idaho Falls, ID.

McElroy, D.L., S.A. Rawson, J.M. Hubbell, S.C. Minkin, R.G. Baca, M.J. Vigil, C.J. Bonzon, J.L. Landon, P.T. Laney, J.R. Pittman, S.R. Anderson, and L.C. Davis. 1989. Site Characterization Program at the Radioactive Waste Management Complex of the Idaho National Engineering Laboratory—Annual progress report, FY-1988 (draft). DOE/ID-10233(88). EG&G Idaho, Inc., Idaho Falls, ID.

Miller, D.E., and W.H. Gardner. 1962. Water infiltration into stratified soil. Soil Sci. Soc. Am. Proc. 26:115–119.

Morse, L.H., and M. McCurry. 1997. Possible correlations between basalt alteration and the effective base of the Snake River Plain aquifer at the INEEL. p. 1–13 *In* Proceedings, Symposium on engineering geology and geotechnical engineering, 32nd, Boise, ID. 26–28 Mar. 1997. .

Nace, R.L., P.T. Voegeli, J.R. Jones, and M. Deutsch. 1975. Generalized geologic framework of the National Reactor Testing Station, Idaho. USGS Professional Paper 725-B. USGS, Idaho Falls, ID.

Nelson, D.M., W.R. Penrose, J.O. Karttunen, and P. Mehlhaff. 1985. Effects of dissolved organic carbon on the adsorption properties of plutonium in natural waters. Environ. Sci. Technol. 19:127–131.

Newman, M.E., I. Porro, R. Scott, F.M. Dunnivant, R.W. Goff, M.D. Blevins, S.M. Ince, J.D. Leyba, T.A. DeVol, A.W. Elzerman, and R.A. Fjeld. 1995. Evaluation of the mobility of Am, Cs, Co, Pu, Sr, and U through INEL basalt and interbed materials—Summary Rep. of the INEL/Clemson University laboratory studies. ER-WAG7-82, INEL-95/282.

Nimmo, J.R., K.S. Perkins, P.A. Rose, J.P. Rousseau, B.R. Orr, B.V. Twining, and S.R. Anderson. 2002. Kilometer-scale rapid transport of naphthalene sulfonate tracer in the unsaturated zone at the Idaho National Engineering and Environmental Laboratory. Vadose Zone J. Available online at www.vadosezonejournal.org. 1:89–101.

Nimmo, J.R., S.M. Shakofsky, J.F. Kaminsky, and G.S. Lords. 1999. Laboratory and field hydrologic characterization of the shallow subsurface at an Idaho National Engineering and Environmental Laboratory waste-disposal site. USGS Water Resources Investigations Rep. 99-4263. USGS, Idaho Falls, ID.

Nimmo, J.R., D.A. Stonestrom, and K.C. Akstin. 1994. The feasibility of recharge rate determinations using the steady-state centrifuge method. Soil Sci. Soc. Am. J. 58:49–56.

Nuttall, H.E., R. Jain, and Y. Fertelli. 1991. Radiocolloid transport in saturated and unsaturated fractures. p. 189–196. *In* Proceedings of the 2nd Annual International Conference on High Level Radioactive Waste Management, Las Vegas, NV.

Nyhan, J.W., B.J. Drennon, W.V. Abeele, M.L. Wheeler, W.D. Purtymun, G. Trujillo, W.J. Herrera, and J.W. Booth. 1985. Distribution of plutonium and americium beneath a 33-yr-old liquid waste disposal site. J. Environ. Qual. 14:501–508.

Orr, B.R. 1999. A Transient Numerical Simulation of Perched Ground-Water Flow at the Test Reactor Area, Idaho National Engineering and Environmental Laboratory, Idaho, 1952–94. USGS Water Resources Investigations Rep. 99-4277. USGS, Idaho Falls, ID.

Parlange, J.Y., and D.E. Hillel. 1976. Theoretical analysis of wetting front instability in soils. Soil Sci. 122:236–239.

Payne, T.E., R. Edis, and T. Seo. 1992. Radionuclide transport by groundwater colloids at the Koongarra uranium deposit. p. 481–488. *In* Proceedings, Material Resource Society Symposium, Vol. 257.

Penrose, W.R., W.L. Polzer, E.H. Essington, D.M. Nelson, and K.A. Orlandini. 1990. Mobility of plutonium and americium through a shallow aquifer in a semiarid region. Environ. Sci. Technol. 24: 228–234.

Perkins, K.S. 2000. Hydrologic and meteorological data for an unsaturated-zone study area near the Radioactive Waste Management Complex, Idaho National Engineering and Environmental Laboratory, Idaho, 1997 to 1999. USGS Open-File Rep. 00-248. USGS, Idaho Falls, ID.

Perkins, K.S. 2003. Measurement of sedimentary interbed hydraulic properties and their hydrologic influence near the Idaho Nuclear Technology and Engineering Center at the Idaho National Engineering and Environmental Laboratory. USGS Water Resources Investigations Rep. 03-4048. USGS, Idaho Falls, ID.

Perkins, K.S., and J.R. Nimmo. 2000. Measurement of hydraulic properties of the B-C interbed and their influence on contaminant transport in the unsaturated zone at the Idaho Engineering and Environmental Laboratory, Idaho. USGS Water Resources Investigations Rep. 00-4073. USGS, Idaho Falls, ID.

Pittman, J.R. 1989. Hydrological and meteorological data for an unsaturated zone study near the Radioactive Waste Management Complex, Idaho National Engineering Laboratory, Idaho—1985–86. USGS Open-File Rep. 98-74. USGS, Idaho Falls, ID.

Pittman, J.R. 1995. Hydrological and meteorological data for an unsaturated-zone study area near the Radioactive Waste Management Complex, Idaho National Engineering Laboratory, Idaho, 1988 and 1989. U.S. Department of Energy. USGS Open-File Rep. 95-112. USGS, Idaho Falls, ID.

Pittman, J.R., R.G. Jensen, and P.R. Fischer. 1988. Hydrologic conditions at the Idaho National Engineering Laboratory, 1982 to 1985. USGS Water Resources Investigations Rep. 89-4008. USGS, Idaho Falls, ID.

Raats, P.A.C. 1973. Unstable wetting fronts in uniform and nonuniform soils. Soil Sci. Soc. Am. Proc. 37:681–685.

Ramsay, J.D.F. 1988. The role of colloids in the release of radionuclides from nuclear waste. Radiochim. Acta 44/45:165–170.

Rathburn, S.L. 1993. Pleistocene cataclysmic flooding along the Big Lost River, east-central Idaho. Geomorphology 8:305–319.

Rawson, S.A., and J.M. Hubbell. 1989. Geochemical controls on the composition of soil pore waters beneath a mixed waste disposal site in the unsaturated zone. p. 241–247. *In* Proceedings, FOCUS '89, Nuclear waste isolation in the unsaturated zone. American Nuclear Society, Las Vegas, NV.

Rawson, S.A., J.C. Walton, and R.G. Baca. 1991. Migration of actinides from a transuranic waste disposal site in the vadose zone. Radiochim. Acta 53:477–486.

Reardon, E.J. 1981. Kds—Can they be used to describe reversible ion sorption reaction in contaminant migration? Ground Water 19:279–286.

Reed, M.F., and R.C. Bartholomay. 1994. Mineralogy of selected sedimentary interbeds at or near the Idaho National Engineering Laboratory, Idaho. U.S. Geological Survey Open-File Rep. 94-374. USGS, Idaho Falls, ID.

Reed, M.F., R.C. Bartholomay, and S.S. Hughes. 1997. Geochemistry and stratigraphic correlation of basalt lavas beneath the Idaho Chemical Processing Plant, Idaho National Engineering Laboratory. Environ. Geol. 30:108–118 p.

Rees, T.F., and J.M. Cleveland. 1982. Characterization of plutonium in waters at Maxey Flats, Kentucky and near the Idaho Chemical Processing Plant, Idaho. p. 41–52. Environmental migration of long-lived radionuclides. IAEA-SM-257/66. International Atomic Energy Agency, Vienna.

Rightmire, C.T. 1984. Description and hydrogeologic implications of cored sedimentary material from the 1975 drilling program at the Radioactive Waste Management Complex, Idaho. USGS Water Resources Investigations Rep. 84-4071 (IDO-22067). USGS, Idaho Falls, ID.

Rightmire, C.T., and B.D. Lewis. 1987a. Geologic data collected and analytical procedures used during a geochemical investigation of the unsaturated zone, Radioactive Waste Management Complex, Idaho National Engineering Laboratory, Idaho. USGS Open File Rep. 87-246. USGS, Idaho Falls, ID.

Rightmire, C.T., and B.D. Lewis. 1987b. Hydrogeology and geochemistry of the unsaturated zone, Radioactive Waste Management Complex, Idaho National Engineering Laboratory, Idaho. USGS Water Resources Investigations Rep. 87-4198. USGS, Idaho Falls, ID.

Robertson, J.B. 1974. Digital modeling of radioactive and chemical waste transport in the Snake River Plain aquifer at the National Reactor Testing Station, Idaho. USGS Open-File Rep. (IDO-22054). USGS, Idaho Falls, ID.

Robertson, J.B., R. Schoen, and J.T. Barraclough. 1974. The influence of liquid waste disposal on the geochemistry of water at the National Reactor Resting Station, Idaho, 1952–1970. USGS Open-File Rep. 73-238 (IDO-22053). USGS, Idaho Falls, ID.

Rousseau, J.P., J.R. Nimmo, S.R. Anderson, R.C. Bartholomay, L.L. Knobel, L.D. Cecil, E.R. Landa, G.P. Curtis, P.D. Glynn, K.G. Stollenwerk, E.M. Kwicklis, C.R. Bossong, and B.R. Orr. 2004. Review of the transport of selected radionuclides in the Interim Risk Assessment for the Radioactive Waste Management Complex, Waste Area Group 7, Operable Unit 7-13/14, Idaho National Engineering and Environmental Laboratory, Idaho. USGS Water Resources Investigation Rep. (In press.) INEEL, Idaho Falls, ID.

Seitz, M.G., P.G. Rickert, S.M. Fried, A.M. Friedman, and M.J. Steindler. 1978. Studies of nuclear-waste migration in geologic media. ANL-78-8. Illinois.

Shakofsky, S.M. 1995. Changes in soil hydraulic properties caused by construction of a simulated waste trench at the Idaho National Engineering Laboratory, Idaho. USGS Water Resources Investigations Rep. 95-4058. USGS, Idaho Falls, ID.

Shakofsky, S.M., and J.R. Nimmo. 1996. Unsaturated zone properties at a waste disposal site at the Idaho National Engineering Laboratory. p. 949–953. *In* D.W. Morganwalp and D.A. Aronson (ed.) U.S. Geological Survey Toxic Substances Hydrology Program–Proceedings of the Technical Meeting, Colorado Springs, CO. 20–24 Sept. 1993. USGS Water Resources Investigations Rep. 94-4015.

Sheppard, J.C., M.J. Campbell, T. Cheng, and J.A. Kittrick. 1980a. Retention of radionuclides by mobile humic compounds and soil particles. Environ. Sci. Technol. 14:1349–1353.

Sheppard, J.C., M.J. Campbell, J.A. Kittrick, and T. Cheng. 1980b. Investigation of the transport of actinide-bearing soil colloids in the soil-aquatic environment. U.S. Department of Energy. DOE/EV/73012–5. Variously p.

Sheppard, J.C., and J.A. Kittrick. 1983. Factors influencing the transport of actinides in the groundwater environment. DOE/EV/7312-2. USDOE, Washington, DC.

Smith, R.P. 2004. Geologic setting of the Snake River Plain aquifer and vadose zone. Available at www.vadosezonejournal.org. Vadose Zone J. 3:47–58 (this issue).

Stothoff, S.A. 1997. Sensitivity of long-term bare soil infiltration simulations to hydraulic properties in an arid environment. Water Resour. Res. 33: 547–558.

Stout, M.Z., and J. Nichols. 1977. Mineralogy and petrology of Quaternary lavas from the Snake River Plain, Idaho. Can. J. Earth Sci. 14:2140–2156.

Su, G.W., J.T. Geller, K. Pruess, and F. Wen. 1999. Experimental studies of water seepage and intermittent flow in unsaturated, rough-walled fractures. Water Resour. Res. 35:1019–1037.

Tokunaga, T., and J. Wan. 1997. Water film flow along fracture surfaces of porous rock. Water Resour. Res. 33:1287–1295.

Tucker, B.J., and B.R. Orr. 1998. Distribution of selected radiochemical and chemical constituents in water from perched ground water. Idaho National Engineering Laboratory, Idaho, 1989–91. USGS Water Resources Investigations Rep. 98-4028 (DOE/ID-22144). USGS, Idaho Falls, ID.

Vilks, P., F. Caron, and M.K. Haas. 1998. Potential for the formation and migration of colloidal material from a near-surface waste disposal site. Appl. Geochem. 13:31–42.

Vilks, P., and D.J. Drew. 1986. The effects of colloids on actinide migration. p. 667–673. *In* Proceedings 2nd International Conference on Radioactive Waste Management, Winnipeg, Manitoba. 7–11 Sept. 1986. Canadian Nuclear Society, Toronto.

Welhan, J., T. Funderberg, R.P. Smith, and A. Wylie. 1997. Stochastic modeling of hydraulic conductivity in the Snake River Plain aquifer: 1. Hydrologeologic constraints and conceptual approach. p. 75–91. *In* S. Sharma and J.H. Hardcastle (ed.) Proceedings, Symposium on Engineering Geology and Geotechnical Engineering, Boise, ID. 26–28 Mar. 1997. Idaho State University, Pocatello.

Welhan, J.A., T.M. Clemo, and E.L. Gégo. 2002a. Stochastic simulation of aquifer heterogeneity in a layered basalt aquifer system, eastern Snake River Plain, Idaho. p. 225–247. *In* P.K. Link and L.L. Mink (ed.) Geology, hydrogeology, and environmental remediation—Idaho National Engineering and Environmental Laboratory, Eastern Snake River Plain, Idaho. Special Paper 353. Geological Society of America, Boulder, CO.

Welhan, J.A., C.M. Johannesen, K.S. Reeves, T.M. Clemo, J.A. Glover, and K.W. Bosworth. 2002b. Morphology of inflated pahoehoe lavas and spatial architecture of their porous and permeable zones, eastern Snake River Plain. Idaho. p. 135–150. *In* P.K. Link and L.L. Mink (ed.) Geology, hydrogeology, and environmental remediation—Idaho National Engineering and Environmental Laboratory, Eastern Snake River Plain, Idaho. Special Paper 353. Geological Society of America, Boulder, CO.

Winfield, K.A. 2003. Spatial variability of sedimentary interbed properties near the Idaho Nuclear Technology and Engineering Center at the Idaho National Environmental and Engineering Laboratory. USGS Water Resources Investigations Rep. 03-4142. USGS, Denver, CO.

Wood, T.R., and G.T. Norrell. 1996. Integrated large-scale aquifer pumping and infiltration tests, groundwater pathways. Summary Rep. OU 7–06 INEL-96/0256. Lockheed Martin Idaho Technologies Company, Idaho Falls, ID.

Wood, W.W., and W.H. Low. 1986. Aqueous geochemistry and diagenesis in the Eastern Snake River Plain aquifer system, Idaho. Geol. Soc. Am. Bull. 97:1456–1466.